Acta Neuropathologica Communications

RESEARCH

Open Access

# Rotenone targets midbrain astrocytes to produce glial dysfunction-mediated dopaminergic neurodegeneration

Ikuko Miyazaki[1*], Nami Isooka[1], Ryo Kikuoka[1,2], Fuminori Imafuku[1], Kaori Masai[1], Kana Tomimoto[1], Masakiyo Sakaguchi[3], Chiharu Sogawa[4], Norio Sogawa[1,5], Yoshihisa Kitamura[6] and Masato Asanuma[1]

## Abstract

Exposure to pesticides, such as rotenone or paraquat, is an environmental factor that plays an important role in the pathogenesis of Parkinson's disease (PD). Rotenone induces PD-like pathology and is therefore used to develop parkinsonian animal models. Dopaminergic neurotoxicity caused by rotenone has been attributed to the inhibition of mitochondrial complex I, oxidative stress and neuroinflammation; however, the mechanisms underlying selective dopaminergic neurodegeneration by rotenone remain unclear. To resolve this, we focused on glial diversity and examined whether the brain region-specific glial response to rotenone could determine the vulnerability of dopaminergic neurons using primary cultured neurons, astrocytes and microglia from the midbrain and striatum of rat embryos and rotenone-injected PD model mice. Direct neuronal treatment with low-dose rotenone failed to damage dopaminergic neurons. Conversely, rotenone exposure in the presence of midbrain astrocyte and microglia or conditioned media from rotenone-treated midbrain glial cultures containing astrocytes and microglia produced dopaminergic neurotoxicity, but striatal glia did not. Surprisingly, conditioned media from rotenone-treated midbrain astrocytes or microglia monocultures did not affect neuronal survival. We also demonstrated that rotenone targeted midbrain astrocytes prior to microglia to induce dopaminergic neurotoxicity. Rotenone-treated astrocytes produced secreted protein acidic and rich in cysteine (SPARC) extracellularly, which induced microglial proliferation, increase in IL-1β and TNF-α, and NF-κB (p65) nuclear translocation in microglia, resulting in dopaminergic neurodegeneration. In addition, rotenone exposure caused the secretion of NFAT-related inflammatory cytokines and a reduction in the level of an antioxidant metallothionein (MT)-1 from midbrain glia. Furthermore, we observed microglial proliferation and a decrease in the number of MT-positive astrocytes in the substantia nigra, but not the striatum, of low-dose rotenone-injected PD model mice. Our data highlight that rotenone targets midbrain astrocytes, leading to SPARC secretion, which promotes the neurotoxic conversion of microglia and leads to glial dysfunction-mediated dopaminergic neurodegeneration.

**Keywords** Rotenone, Astrocyte, Microglia, SPARC, Parkinson's disease

*Correspondence:
Ikuko Miyazaki
miyazaki@cc.okayama-u.ac.jp

Full list of author information is available at the end of the article

## Introduction

Parkinson's disease (PD) is a progressive neurodegenerative disease characterized by motor symptoms, such as tremor, bradykinesia, rigidity, and postural instability due to a loss of nigrostriatal dopaminergic neurons; and non-motor symptoms, such as orthostatic hypotension and constipation caused by peripheral neurodegeneration. The cause of sporadic PD remains unknown, and genetic and environmental factors may be contributing factors. Epidemiological studies indicate that exposure to pesticides, particularly rotenone and paraquat, increases the risk of PD [16]. Studies have shown that rotenone, a mitochondrial complex I inhibitor, induces PD-like features and is therefore used to develop animal models of PD [11, 22]. Dopaminergic neurotoxicity caused by rotenone has been attributed, in part, to the inhibition of complex I activity and the vulnerability of dopaminergic neurons to complex I defects [11]. Moreover, oxidative stress is thought to be involved in rotenone neurotoxicity because rotenone-induced complex I inhibition produces reactive oxygen species (ROS) [10, 47]. However, the mechanism underlying rotenone-induced selective dopaminergic neurodegeneration remains unknown.

Glial cells, namely astrocytes and microglia, have received attention as key players in non-cell autonomous pathological mechanisms in neurodegenerative diseases [12, 28]. Astrocytes play important roles in the central nervous system (CNS), such as providing energy substrates for neurons, regulating extracellular ion concentrations, removing or releasing neurotransmitters, and modulating synaptic transmission [37]. In addition, studies have demonstrated the neuroprotective effects of astrocytes via antioxidant production, neurotrophic factor release, and the uptake of potentially neurotoxic molecules [32, 42, 49]. To date, the function of astrocytes under pathological conditions has been debated. Studies have shown the neurotoxic effects of astrocytes in neurodegeneration, in which the cells secrete cytokines and inflammatory mediators [20]. Conversely, various studies, including our group, have demonstrated a neuroprotective function of astrocytes through the production of antioxidative molecules [3, 32]. Microglia survey the brain microenvironment and play important roles in removing neuronal debris and protein aggregates for neuroprotection [23]. Under stimulation, microglia can change their morphology and release inflammatory cytokines [43]. Recent studies have demonstrated crosstalk and cooperation between astrocytes and microglia in neuroinflammation; activated microglia convert astrocytes into neurotoxic A1 astrocytes in neurological diseases [27].

Astrocytes or microglia are morphologically and functionally diverse and glial reactivity varies according to brain region [8, 29]. In addition, the diverse roles of glial cells include modulating neuronal survival via neuron-glia interactions. In this study, we focused on regional differences in glial reactivity to explore the mechanism of rotenone-induced dopaminergic neurotoxicity. We examined the effect of glial diversity on vulnerability of dopaminergic neurons to rotenone by using midbrain neurons and midbrain or striatal glial cells containing astrocytes and microglia. These regions were chosen, because the cell bodies of dopaminergic neurons are present in the substantia nigra pars compacta (SNpc) and their axons extend to the striatum. In this study, cultured cells were treated with low-dose rotenone (1, 2.5, or 5 nM) for 48 h to mimic environmental exposure. We demonstrated here that direct neuronal treatment with low-dose rotenone did not induce dopaminergic neurotoxicity. However, conditioned media from rotenone-treated midbrain, but not striatal, glial cells (astrocytes + microglia) induced dopaminergic neuron-specific neurodegeneration. The conditioned media from rotenone-treated astrocyte or microglial monocultures could not induce dopaminergic neurotoxicity. Furthermore, rotenone targeted midbrain astrocytes prior to microglia, leading to the production of secreted protein acidic and rich in cysteine (SPARC), which induced neurotoxic conversion of microglia followed by dopaminergic neuronal death. Through astrocyte-microglia crosstalk, rotenone exposure caused the secretion of inflammatory cytokines and decreased the production of the antioxidant molecule metallothionein (MT)-1 from/in midbrain, but not striatal, glial cells; these results suggest that rotenone induced brain region-specific glial dysfunction. We also detected microglial proliferation and a reduction in the number of MT-expressing astrocytes in the SNpc, but not in the striatum, of low-dose rotenone-injected PD model mice. This study unveils a novel mechanism of rotenone-induced dopaminergic neuron-specific neurotoxicity.

## Methods

### Animals

All experimental procedures were conducted in accordance with the NIH Guide for the Care and Use of Experimental Animals and the Policy on the Care and Use of the Laboratory Animals, Okayama University, and were approved by the Animal Care and Use Committee, Okayama University (approval reference numbers: OKU-2017058, OKU-2017059, OKU-2020004, OKU-2020005, OKU-2023032 and OKU-2023033). Pregnant Sprague–Dawley (SD) rats at 13 days of gestation were purchased from Charles River Japan Inc. (Yokohama, Japan) for primary culture and housed for 2 days. Male and female homozygous MT-1,2 knockout mice (#2211: 129S7/SvEvBrd-MT1$^{tm1Bri}$MT2$^{tm1Bri}$/J) and 129/Sv mice (wild-type mice) (#2448: 129S1/SvImJ) were purchased from Jackson Laboratories (Bar Harbor, ME). The 129/Sv mice

were used as control mice to match the genetic background of the MT-1,2 knockout mice. Male C57BL/6 J mice at 7 weeks of age were purchased from Charles River Japan Inc. All the animals were housed with a 12-h light/dark cycle at a constant temperature (23 °C) and ad libitum access to food and water.

#### Cell culture

Primary cultured neurons, astrocytes and microglia were prepared from the mesencephalon and striata of SD rats, MT-1,2 knockout mice or wild-type mice embryos at 15 days of gestation using the method described previously [21, 33]. Briefly, to prepare midbrain neuronal cultures (Mid neuron), the mesencephalon was dissected and cut into small pieces with scissors. The tissue was incubated for 15 min in 0.125% trypsin–EDTA at 37 °C and then centrifuged (1500×*g*, 3 min). The resulting cell pellet was treated with 0.004% DNase I solution containing 0.003% trypsin inhibitor for 7 min at 37 °C and then centrifuged (1500×*g*, 3 min). The resulting cell pellet was gently re-suspended in a small volume of Dulbecco's modified Eagle's medium (DMEM) with high glucose (4.5 g/l D-glucose; Invitrogen, San Diego, CA, USA) containing 10% fetal bovine serum (FBS), 4 mM L-glutamine, and 60 mg/l kanamycin sulfate (growth medium; DMEM–FBS) and plated in the same medium at a density of $2 \times 10^5$ cells/cm$^2$ in 4-chamber culture slides or 6-well plates coated with poly-D-lysine (Falcon, Corning, NY, USA). Within 24 h of initial plating, the medium was replaced with fresh DMEM-FBS supplemented with 2 μM cytosine-β-D-arabinofuranoside (Ara-C) to inhibit glial cell replication, followed by incubation for 6 days.

To prepare midbrain or striatal glial cultures (Mid glia or Str glia) containing astrocytes and microglia, the mesencephalon or striata were dissected and treated with 0.125% trypsin followed by 0.004% DNase I solution as described above. The cells from the mesencephalon or striata were plated at a density of $2 \times 10^5$ cells/cm$^2$ in poly-D-lysine-coated 6-well plates and cultured for 7 days in DMEM-FBS. Next, the cells were subcultured to obtain glial cells and plated at a density of $3.6 \times 10^4$ cells/cm$^2$ onto 6-well plates (Falcon) for preparation of the conditioned media, complex I activity assay, or protein extraction; at a density of $3.6 \times 10^4$ cells/cm$^2$ onto 24-well plates for immunohistochemical analysis; at a density of $2 \times 10^4$ cells/cm$^2$ onto four-chamber glass culture slides coated with poly-D-lysine (Falcon) for immunohistochemical analysis; or at a density of $2 \times 10^4$ cells/cm$^2$ onto 96-well culture plates (Falcon) for ATP assay. After 7 days of culture, the Mid glia contains 87.7% astrocytes and 12.3% microglia; the Str glia contains 98.6% astrocytes and 1.4% microglia. Oligodendrocyte marker proteins were not detected in glial cultures.

To prepare cocultures of midbrain neurons and midbrain or striatal glia (Mid neuron + Mid glia or Mid neuron + Str glia), glial cells were seeded at a density of $4 \times 10^4$ cells/cm$^2$ directly onto Mid neuron, which had been cultured in 4-chamber culture slides for 4 days. The cocultures were incubated for an additional 2 days before any treatment was started.

To prepare midbrain or striatal astrocyte cultures (Mid astrocyte or Str astrocyte), microglia were eliminated from glial culture by incubation in DMEM-FBS supplemented with 8 μM Ara-C for 5 days, followed by treatment with 30 mM L-leucine methyl ester hydrochloride for 45 min [19]. After 1 day of culture, more than 99.9% of the cells presented astrocytic marker proteins.

To prepare midbrain or striatal microglial cultures (Mid microglia or Str microglia), the mesencephalon or striata were treated with 0.125% trypsin followed by 0.004% DNase I solution, and then cultured in 6-well plates for 12–14 days. Microglia were isolated by shaking and collecting floating cells [21]. The cells were re-plated at a density of $3.6 \times 10^4$ cells/cm$^2$ onto 6-well plates, or at a density of $2 \times 10^4$ cells/cm$^2$ onto four-chamber culture slides coated with poly-D-lysine. After 1 day of culture, all the cells presented microglial marker proteins.

To prepare astrocyte and microglia cocultures which abundance ratio of astrocytes and microglia was adjusted to that of Mid glia or Str glia, midbrain microglia were seeded at a density of $1.2 \times 10^4$ cells/cm$^2$ or $1.1 \times 10^3$ cells/cm$^2$ directly onto Mid astrocyte ($8.7 \times 10^4$ cells/cm$^2$) for astrocyte (88%) and microglia (12%) coculture or astrocyte (98.8%) and microglia (1.2%) coculture, respectively; striatal microglia were seeded at a density of $1.5 \times 10^4$ cells/cm$^2$ or $1.4 \times 10^3$ cells/cm$^2$ directly onto Str astrocyte ($11.3 \times 10^4$ cells/cm$^2$) for astrocyte (88%) and microglia (12%) coculture or astrocyte (98.8%) and microglia (1.2%) coculture, respectively. All the cultures were maintained at 37 °C in a 5–95% $CO_2$-air gas mixture.

#### Preparation of conditioned medium

Rotenone (Sigma-Aldrich, St. Louis, MO, USA) was freshly prepared in dimethylsulfoxide (DMSO) for each experiment and then diluted to final concentrations in the medium (final concentration of DMSO: 0.005% (*v*/*v*)). Glial conditioned medium (GCM) was collected from Mid glia or Str glia treated with rotenone (1, 2.5, or 5 nM; Rotenone-GCM) or vehicle (0.005% (*v*/*v*) DMSO; Control-GCM) for 48 h in DMEM-FBS. To measure cytokines and antioxidants in GCM, the cells were treated with rotenone (1, 2.5, or 5 nM) or vehicle for 48 h in serum-free DMEM. The astrocyte or microglial conditioned medium (ACM or MCM) was collected from Mid or Str astrocyte or microglia after treatment with rotenone (5 nM; Rotenone-ACM or Rotenone-MCM) or vehicle (Control-ACM or Control-MCM) in DMEM-FBS

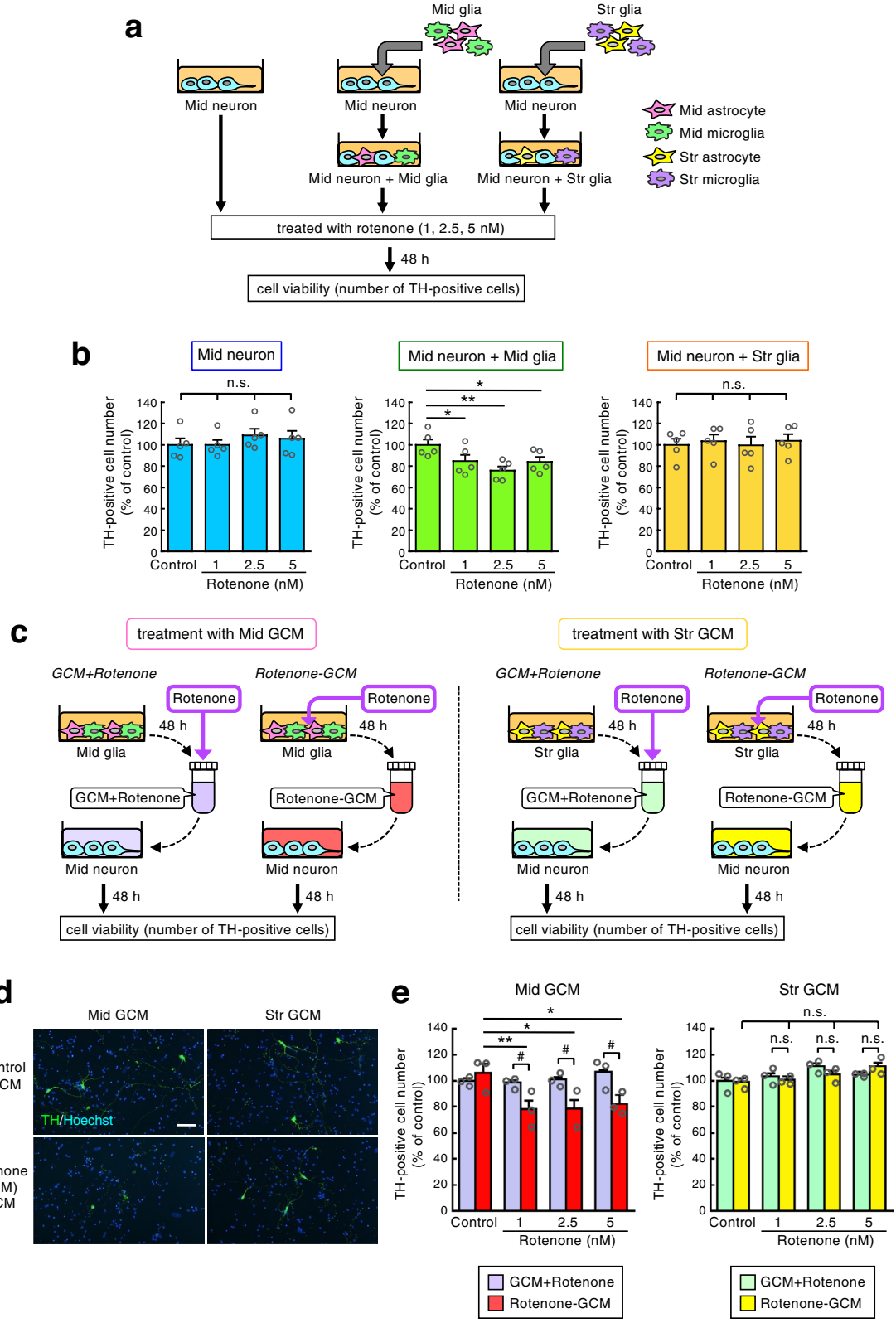


**Fig. 1** (See legend on next page.)

(See figure on previous page.)

**Fig. 1** Midbrain, but not striatal, glia mediate rotenone-induced dopaminergic neurodegeneration. **a** Schematic illustration of cell culture and rotenone treatment. Mid neuron, Mid neuron + Mid glia, or Mid neuron + Str glia was treated with vehicle or rotenone (1, 2.5, or 5 nM) for 48 h, and then TH-positive cells were counted. **b** Cell viability of TH-positive dopaminergic neurons, expressed as a percentage of the control. *$p < 0.05$, **$p < 0.01$ versus control group. n.s., not significant. **c** Schematic illustration of cell treatment. The GCM was collected from vehicle- or rotenone (1, 2.5 or 5 nM)-treated Mid glia or Str glia for 48 h (Control- or Rotenone-GCM). GCM + Rotenone: rotenone was added to GCM directly at the same concentration as control. Cell viability of dopaminergic neurons was analyzed after treatment with Rotenone-GCM or GCM + Rotenone for 48 h. **d** Representative images of TH immunostaining in Mid neuron after treatment with Mid or Str Control- or Rotenone (5 nM)-GCM for 48 h. Green, TH-positive neurons. Blue, nuclear staining with Hoechst 33342. Scale bar = 50 µm. **e** Cell viability of TH-positive neurons, expressed as a percentage of the control. *$p < 0.05$, **$p < 0.01$ versus Control-GCM, $^{\#}p < 0.05$ versus dose-matched GCM + Rotenone. n.s., not significant. All data represent mean ± SEM, and are analyzed using one-way ANOVA followed by *post-hoc* Fisher's PLSD test.

for 48 h. The conditioned medium (CM) of astrocyte and microglia cocultures was collected from midbrain or striatal astrocytes (88%) and microglia (12%) coculture or astrocytes (98.8%) and microglia (1.2%) coculture after treatment with rotenone (5 nM; Rotenone-CM) or vehicle (Control-CM) in DMEM-FBS for 48 h. The Control- or Rotenone-ACM-MCM was collected from Mid microglia treated with Control- or Rotenone (5 nM)-ACM for 48 h. The Control- or Rotenone-MCM-ACM was collected from Mid astrocyte treated with Control- or Rotenone (5 nM)-MCM for 48 h. The Rotenone-ACM + SPARC Ab-MCM was collected from Mid microglia treated with Rotenone-ACM pre-incubated with a mouse anti-SPARC monoclonal antibody (Ab) (1:500, Santa Cruz) for 1 h at 25 °C. The conditioned media were centrifuged at 3,000 × *g* for 3 min to remove cellular debris, and the supernatants were stored at – 80 °C until use.

#### Cell treatments

To examine the effects of glial cells on rotenone-induced dopaminergic neurotoxicity, Mid neuron, Mid neuron + Mid glia or Mid neuron + Str glia was treated with rotenone (1, 2.5, or 5 nM) or vehicle (0.005% (*v*/*v*) DMSO) in DMEM-FBS for 48 h (Fig. 1a). To examine whether rotenone-induced dopaminergic neurotoxicity was mediated by glial cells, Mid neuron was treated with Control- or Rotenone-GCM for 48 h. To exclude the possibility that rotenone reacting with GCM promoted neuronal damage, we added rotenone to GCM directly at the same concentration (GCM + Rotenone) (Fig. 1c). To examine whether intracellular dopamine (DA) is involved in Rotenone-GCM-induced dopaminergic neurotoxicity, Mid neuron was treated with the tyrosine hydroxylase (TH) inhibitor, α-methyl-*p*-tyrosine (AMPT; 50 µM), for 24 h, which caused DA depletion, and then treated with AMPT (50 µM) and Mid Rotenone (5 nM)-GCM for 48 h (Fig. 2d). To examine whether rotenone-induced dopaminergic neurotoxicity required astrocyte-microglia interaction, Mid neuron was treated with Control- or Rotenone-GCM, ACM or MCM for 48 h (Fig. 3a). To examine whether brain region-specific astrocyte-microglia interaction promoted rotenone-induced dopaminergic neurotoxicity, Mid neuron was treated with Control- or Rotenone-CM from Mid or Str astrocyte (88%) and microglia (12%) coculture or astrocyte (98.8%) and microglia (1.2%) coculture for 48 h. To examine whether rotenone acted first on astrocytes or microglia, Mid neuron was treated with Control- or Rotenone-ACM-MCM or MCM-ACM for 48 h (Fig. 4). To assess the contribution of SPARC secreted from rotenone-treated astrocytes to dopaminergic neurodegeneration, Mid neuron was treated with Control-ACM-MCM, Rotenone-ACM-MCM or Rotenone-ACM + SPARC Ab-MCM (Fig. 5c). To examine whether the reduction in MT-1 secretion from rotenone-treated Mid glia promoted dopaminergic neurotoxicity, Mid neuron was treated with Rotenone-GCM supplemented with rabbit MT-1 recombinant protein (300 pg/ml, ENZO Life Sciences, Farmingdale, NY) (Fig. 7b). To examine whether SPARC secretion from rotenone-treated Mid astrocyte induces microglial toxic conversion, Mid microglia was treated with Control-ACM, Rotenone-ACM or Rotenone-ACM + SPARC Ab for 48 h. Furthermore, we prepared Mid neuron, Mid neuron + Mid glia and Mid neuron + Str glia from embryos of MT-1,2 knockout or wild-type mice; the cells were treated with rotenone (1, 2.5, or 5 nM) in DMEM-FBS for 24 h. To examine molecular events in glial cultures after rotenone treatment, Mid glia or Str glia was treated with rotenone (1, 2.5, or 5 nM) in DMEM-FBS for 6–48 h.

#### Chronic systemic rotenone exposure in mice

Male C57BL/6 J mice (8 weeks old; approximately 25 g) were subcutaneously injected with rotenone (2.5 mg/kg/day) for 4 weeks using an osmotic mini pump (Alzet, #2004; Durect Corporation, Cupertino, CA, USA) [34]. The mean pumping rate of the Alzet osmotic mini pump was 0.25 µl/h (= 6 µl/day). Therefore, the osmotic pump was filled with rotenone (10.4 mg/ml) dissolved in the vehicle solution, which consisted of equal volumes of DMSO and polyethylene glycol. The mice were anesthetized by isoflurane inhalation. A rotenone-filled pump was implanted under the skin on the back of each mouse. The control mouse was implanted with a vehicle solution-filled pump.

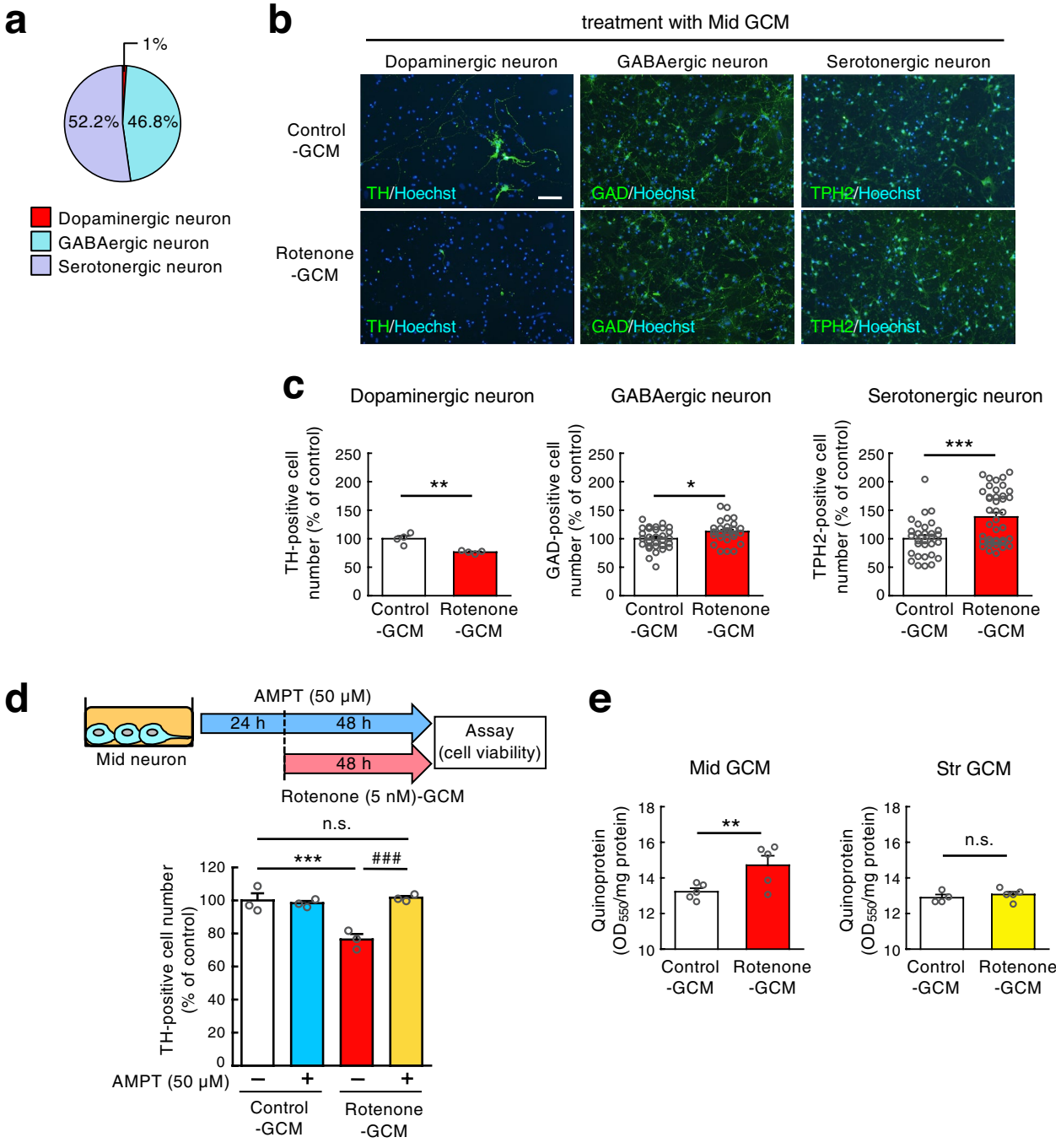


**Fig. 2** Rotenone-exposed midbrain glia increase DA quinone formation in neurons resulting in dopaminergic neuron-specific neurodegeneration. **a** Pie chart showing the neuron subtype composition of Mid neuron. **b** Representative images of TH, GAD, or TPH2 immunostaining in Mid neuron following treatment with Mid Control- or Rotenone (5 nM)-GCM for 48 h. Green, TH-positive dopaminergic, GAD-positive GABAergic, or TPH2-positive serotonergic neurons. Blue, nuclear staining with Hoechst 33342. Scale bar = 50 μm. **c** The number of TH-, GAD-, or TPH2-positive neurons after treatment with Mid Control- or Rotenone (5 nM)-GCM for 48 h, expressed as a percentage of the control. *$p < 0.05$, **$p < 0.01$, ***$p < 0.001$ versus Control-GCM. Statistics were performed by independent *t* test. **d** Effects of DA depletion on Rotenone-GCM-induced dopaminergic neurotoxicity. Top, schematic illustration of cell treatment. The Mid neuron was pre-treated with the TH inhibitor AMPT (50 μM) for 24 h and then co-treated with Mid Control- or Rotenone (5 nM)-GCM for 48 h. Bottom, number of TH-positive neurons, expressed as a percentage of the control. ***$p < 0.001$ versus Control-GCM, $^{\#\#\#}p < 0.001$ versus Rotenone (5 nM)-GCM. n.s., not significant. **e** Quinoprotein levels in Mid neuron after treatment with Mid or Str Control- or Rotenone (5 nM)-GCM. **$p < 0.01$ versus Control-GCM. n.s., not significant. Data (**d**, **e**) are analyzed using one-way ANOVA followed by *post-hoc* Fisher's PLSD test. All data represent mean ± SEM.

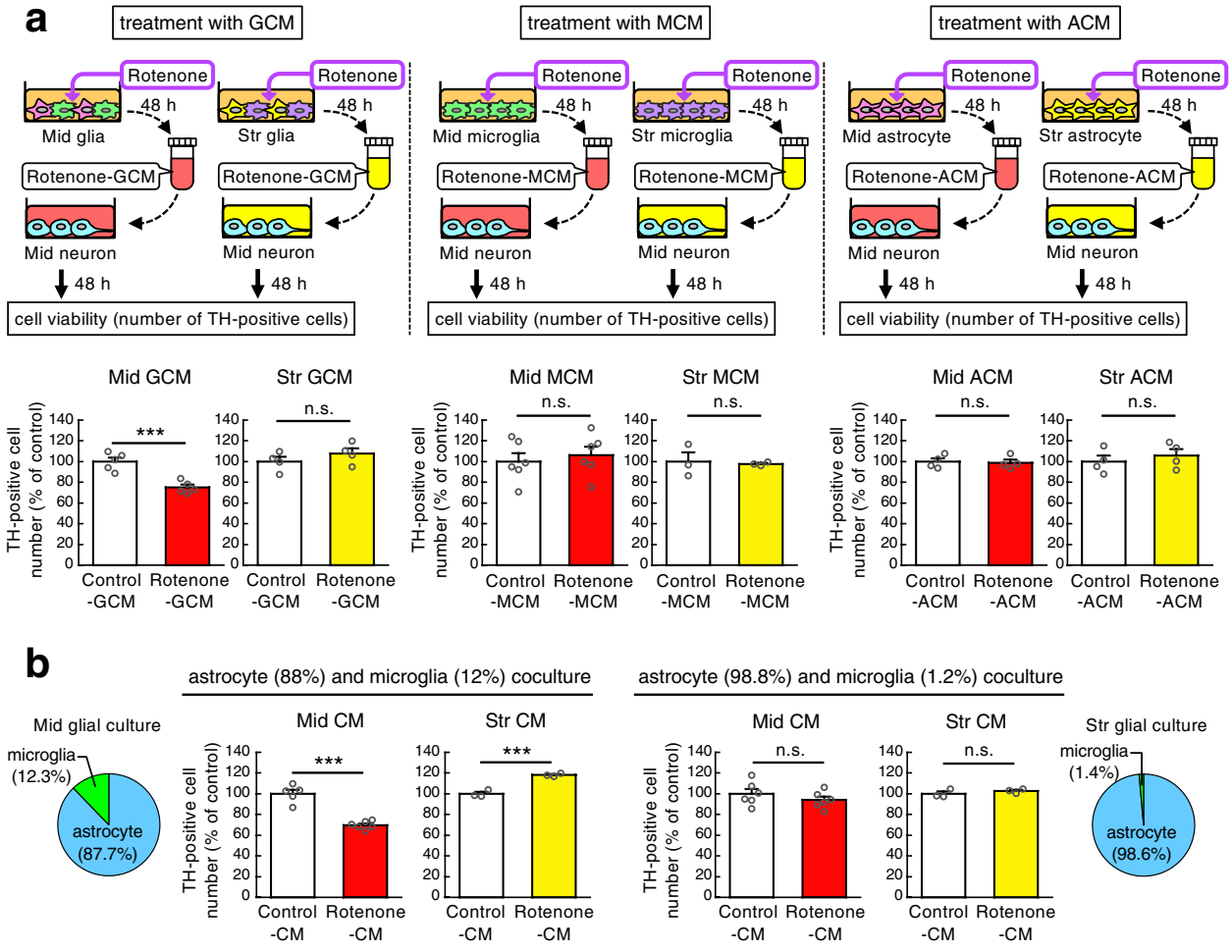


**Fig. 3** Rotenone requires both midbrain astrocytes and microglia to induce dopaminergic neurodegeneration. **a** Cell viability of TH-positive neurons after treatment with Mid or Str Control- or Rotenone (5 nM)-GCM, MCM or ACM. Top, schematic illustration of cell treatment. The GCM, MCM, or ACM was collected from vehicle- or rotenone (5 nM)-treated Mid or Str glia (Control- or Rotenone-GCM), microglia (Control- or Rotenone-MCM) or astrocyte (Control- or Rotenone-ACM) for 48 h, respectively, and then added to Mid neuron. After 48-h treatment, cell viability of dopaminergic neurons was analyzed. Bottom, number of TH-positive neurons, expressed as a percentage of the control. ***$p < 0.001$ versus Control-CM. n.s., not significant. **b** Cell viability of TH-positive neurons after treatment with CM from rotenone (5 nM)-treated midbrain or striatal astrocyte and microglia cocultures. Pie chart showing the abundant proportions of astrocytes and microglia in Mid glia or Str glia. Left, the abundance ratio of astrocyte and microglia was adjusted to that of Mid glia (astrocyte (88%) and microglia (12%)). Right, the abundance ratio of astrocytes and microglia was adjusted to that of Str glia (astrocyte (98.8%) and microglia (1.2%)). The number of TH-positive neurons was expressed as a percentage of the control. ***$p < 0.001$ versus Control-CM. n.s., not significant. All data represent mean ± SEM, and are analyzed using independent *t* test.

### Immunohistochemistry

All the experimental procedures used for immunohistochemistry are thoroughly described in Additional file 1: Materials and Methods. The antibodies and appropriate dilutions used for these methods are listed in Supplementary Table 1.

### Measurement of protein-bound quinone (quinoprotein)

Mid neuron was exposed to Control- or Rotenone (5 nM)-GCM from Mid glia or Str glia for 48 h. Total cell lysates were extracted using ice-cold RIPA buffer (PBS pH 7.4, 1% NP-40, 0.5% sodium deoxycholate, and 0.1% SDS) containing 10 µg/ml phenylmethylsulfonyl fluoride (PMSF). Protein-bound quinones (quinoprotein) in the lysates were detected using the NBT/glycinate assay, as described previously [39], with minor modifications. The detailed experimental procedures are described in Additional file 1: Materials and Methods.

## Secretomics

### Analysis using control- or rotenone-ACM from Mid astrocyte

We analyzed increased proteins in the Mid Rotenone-ACM. Mid astrocyte was treated with vehicle or rotenone (5 nM) for 48 h in serum-free media. The ACM was centrifuged to remove cellular debris, and the supernatants were stored at – 80 °C until use. Aliquots (12 ml) of Control- or Rotenone-ACM were concentrated to 200 µl

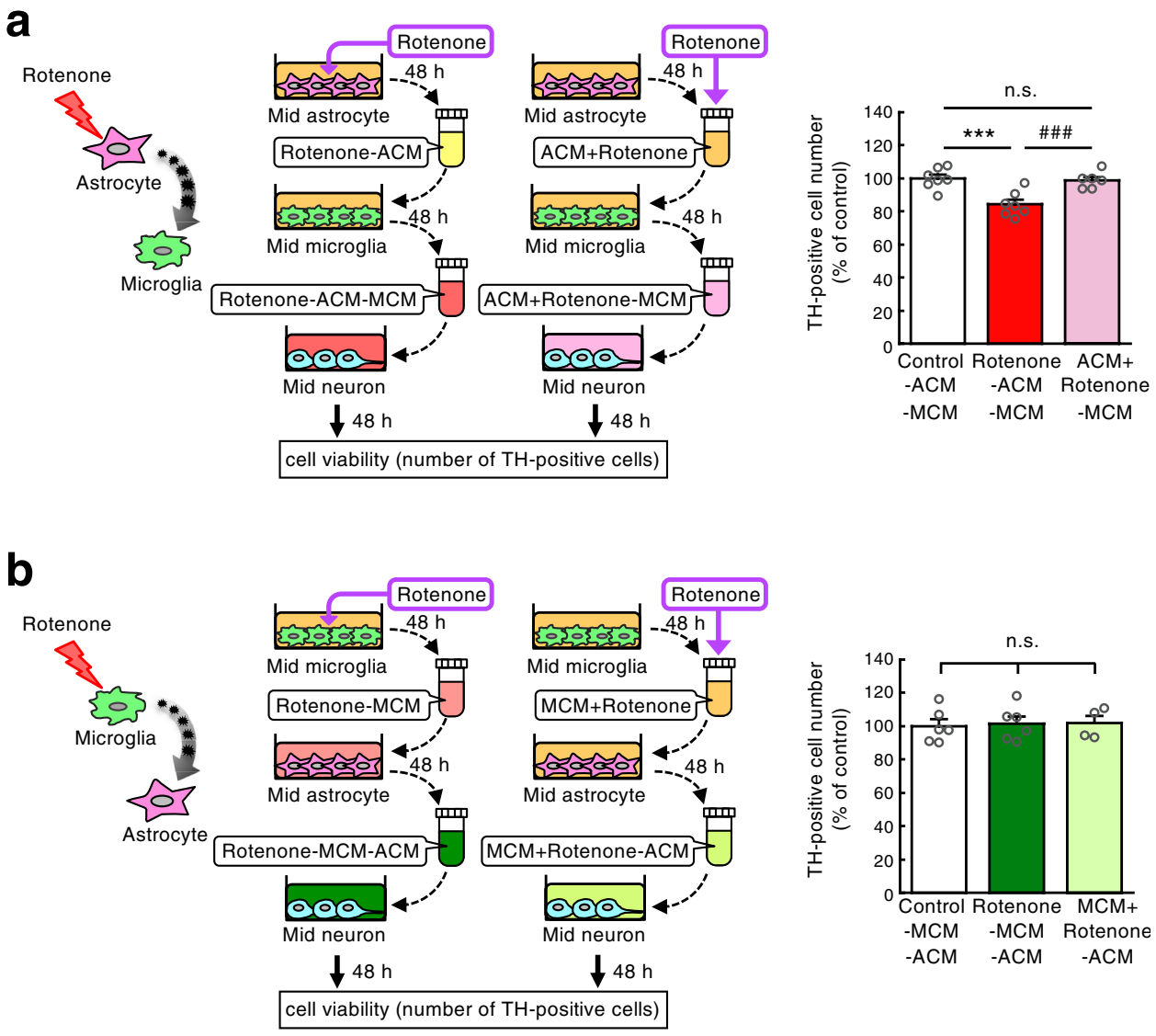


**Fig. 4** Rotenone targets midbrain astrocytes prior to microglia to induce dopaminergic neurodegeneration. **a** Rotenone was added to astrocytes before microglia. Left, schematic illustration of cell treatment. The ACM was collected from vehicle- or rotenone (5 nM)-treated Mid astrocyte for 48 h (Control- or Rotenone-ACM). ACM + Rotenone: rotenone (5 nM) was added to ACM directly as control. The Mid microglia was treated with Control-ACM, Rotenone-ACM or ACM + Rotenone for 48 h, and then the conditioned media were collected as Control-ACM-MCM, Rotenone-ACM-MCM or ACM + Rotenone-MCM, respectively. Cell viability of dopaminergic neurons was analyzed after treatment with Control-ACM-MCM, Rotenone-ACM-MCM or ACM + Rotenone-MCM for 48 h. Right, the number of TH-positive neurons, expressed as a percentage of the control. ***$p < 0.001$ versus Control-ACM-MCM, $^{\#\#\#}p < 0.001$ versus Rotenone-ACM-MCM. n.s., not significant. **b** Rotenone was added to microglia before astrocytes. Left, schematic illustration of cell treatment. The MCM was collected from vehicle- or rotenone (5 nM)-treated Mid microglia for 48 h (Control- or Rotenone-MCM). MCM + Rotenone: rotenone (5 nM) was added to MCM directly as control. The Mid astrocyte was treated with Control-MCM, Rotenone-MCM or MCM + Rotenone for 48 h, and then the conditioned media were collected as Control-MCM-ACM, Rotenone-MCM-ACM or MCM + Rotenone-ACM, respectively. Cell viability of dopaminergic neurons was analyzed after treatment with Control-MCM-ACM, Rotenone-MCM-ACM or MCM + Rotenone-ACM for 48 h. Right, the number of TH-positive neurons, expressed as a percentage of the control. n.s., not significant. All data represent mean ± SEM, and are analyzed using one-way ANOVA followed by post-hoc Fisher's PLSD test.

by using Amicon® Ultra-4 Centrifugal Filter Units (3 kDa cutoff, Merck Millipore Ltd., Co Cork, Ireland). Each sample was dialyzed for desalting, and then lyophilized (Freeze Dryer Model FDU-2110, TOKYO RIKAKIKAI Corporation, Ltd., Tokyo, Japan). The lyophilized samples were re-suspended in sampling buffer (0.1 M Tris–HCl (pH 6.8), 4% SDS, 20% glycerol, 0.02% bromophenol blue-methanol, and 10% 2-mercaptoethanol). Proteins were separated on Any kD SDS-PAGE (Bio-Rad, Richmond, CA, USA) and visualized by silver staining (Silver Stain II Kit Wako, FUJIFILM Wako Pure Chemical Corporation) according to the manufacturer's instructions. Increased bands in the Rotenone-ACM were sliced and in-gel digested with trypsin (Trypsin Profile IGD Kit,

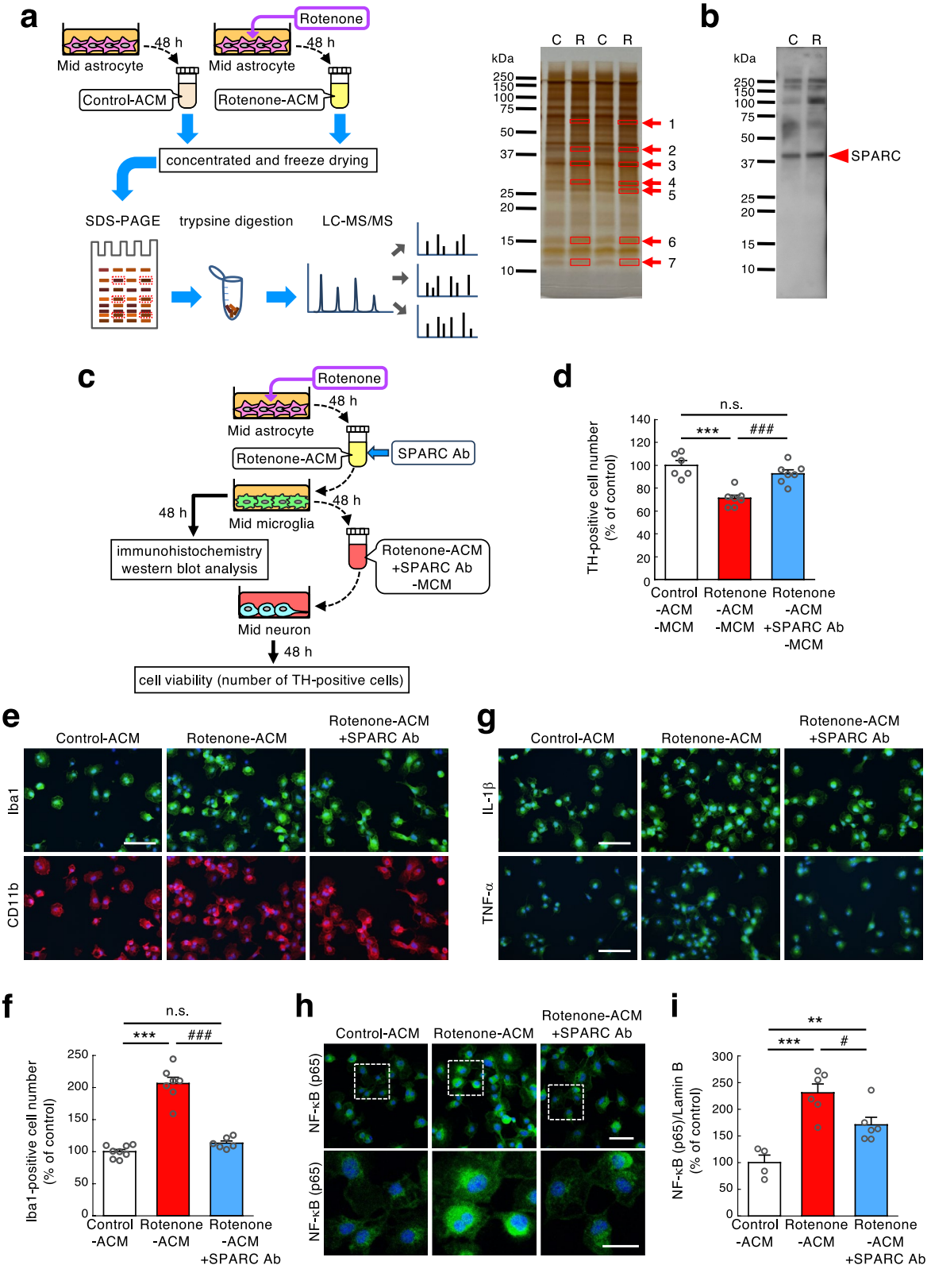


**Fig. 5** (See legend on next page.)

(See figure on previous page.)

**Fig. 5** Midbrain astrocytes secrete SPARC by rotenone exposure and induce toxic conversion of microglia resulting in dopaminergic neurodegeneration. **a** Secretomics of Rotenone-ACM from rotenone-treated Mid astrocyte. Left, schematic illustration of experimental workflow. Control- or Rotenone (5 nM)-ACM was concentrated, and then separated on Any kD SDS polyacrylamide gel. After the gel was silver stained, increased bands in the Rotenone-ACM were clipped. Each band in the gel was digested with trypsin, and the resulting peptides were analyzed by LC-MS/MS. Right, the silver-stained SDS-PAGE gels. Red arrows represent increased proteins in the Rotenone-ACM. Squares (No. 1-7) show clipped bands for LC-MS/MS analysis. **b** Western blot analysis of SPARC using concentrated Control- or Rotenone (5 n)-ACM. The band of SPARC was indicated by red arrowhead. **c**, **d** Absorption of SPARC in Rotenone-ACM by SPARC Ab significantly prevented Rotenone-ACM-MCM-induced dopaminergic neuronal death. **c** Schematic illustration of cell treatment. Mid microglia was treated with Control-ACM, Rotenone (5 nM)-ACM or Rotenone (5 nM)-ACM pre-incubated with anti-SPARC Ab (Rotenone-ACM + SPARC Ab), and then each conditioned medium, Control-ACM-MCM, Rotenone-ACM-MCM or Rotenone-ACM + SPARC Ab-MCM was added to Mid neuron. After 48-h treatment, TH-positive cells were counted. **d** Number of TH-positive neurons, expressed as a percentage of the control. $^{***}p < 0.001$ versus Control-ACM-MCM, $^{\#\#\#}p < 0.001$ versus Rotenone-ACM-MCM. n.s., not significant. **e-i** SPARC secreted from rotenone-treated astrocytes induced toxic conversion of microglia. **e, g** Representative images of Iba1 (green) and CD11b (red) double-immunostaining (**e**) and IL-1β or TNF-α immunostaining (**g**) in Mid microglia after treatment with Control-ACM, Rotenone-ACM or Rotenone-ACM + SPARC Ab for 48 h. Blue, nuclear staining with Hoechst 33342. Scale bar = 50 µm. **f** Changes in the number of Iba-1-positive cells in Mid microglia after treatment with Control-ACM, Rotenone-ACM or Rotenone-ACM + SPARC Ab for 48 h, expressed as a percentage of the control. $^{***}p < 0.001$ versus Control-ACM, $^{\#\#\#}p < 0.001$ versus Rotenone-ACM. n.s., not significant. **h** Representative confocal images of NF-κB (p65) immunostaining in Mid microglia after treatment with Control-ACM, Rotenone-ACM or Rotenone-ACM + SPARC Ab for 48 h at two different magnifications. The bottom panels are high-magnification images of the top panels (squared areas). Blue, nuclear staining with Hoechst 33342. Scale bar = 50 µm (top) or 25 µm (bottom). **i** Western blot analysis of NF-κB (p65) using nuclear fraction of Mid microglia after treatment with Control-ACM, Rotenone-ACM or Rotenone-ACM + SPARC Ab for 48 h. Each value represents the density of the specific protein signal relative to loading control Lamin B, and is presented as a percentage of the control group. $^{**}p < 0.01$, $^{***}p < 0.001$ versus Control-ACM, $^{\#}p < 0.05$ versus Rotenone-ACM. All data represent mean ± SEM, and are analyzed using one-way ANOVA followed by *post-hoc* Fisher's PLSD test.

Sigma-Aldrich). The resulting peptides were analyzed by liquid chromatography-tandem mass spectrometry (LC–MS/MS) (Agilent 1100LC/MSD Trap XCT Ultra, Agilent Technologies, Santa Clara, CA) and identified by searching in the NCBI database within *Rattus norvegicus* species using Spectrum Mill MS Proteomics Workbench software (Agilent Technologies). Proteins were considered on the basis of their molecular weight. A list of identified proteins is provided in Additional file 2.

#### Analysis using control- or rotenone-GCM from Mid glia

We tried to identify secreted proteins increased or decreased only in the Mid Rotenone-GCM from rotenone (5 nM)-exposed Mid glia. Mid glia or Str glia was treated with vehicle or rotenone (5 nM) for 48 h in serum-free media. The GCM was centrifuged, and the supernatants were stored at − 80 °C until use. Aliquots (8 ml for analysis of > 20 kDa; 14 ml for analysis of small-size protein (3–20 kDa)) of Mid or Str Control- or Rotenone-GCM were concentrated, dialyzed, and then lyophilized. The samples re-suspended with sampling buffer were separated on 4–20% SDS-PAGE (Bio-Rad) and visualized by silver staining. The increased or decreased bands only in the Mid Rotenone-GCM were in-gel digested with trypsin, and then analyzed by LC–MS/MS. The proteins were characterized with LC–MS/MS and identified by searching in the NCBI database. Proteins were considered on the basis of their molecular weight. A list of identified proteins is provided in Additional file 3. We selected some increased or decreased proteins that have been reported to be related to neuron-glia interaction or PD pathology.

#### Cytokine antibody array

To identify the expression profiles of multiple cytokines in Rotenone-GCM, a membrane-based cytokine antibody array was used. Mid glia or Str glia was treated with vehicle or rotenone (5 nM) for 48 h in serum-free media. Media were centrifuged, and the supernatants were used for assessment on the RayBio Rat Cytokine Antibody Array 2 (Cat. #ARR-CYT-2, RayBiotech, Inc., Norcross, GA), according to the manufacturer's instructions. The detailed experimental procedures are described in Additional file 1: Materials and Methods.

#### cDNA Microarray

Microarray were used to comprehensively explore changes in gene expression by rotenone treatment (5 nM) for 24 h in Mid glia or Str glia. The detailed experimental procedures are described in Additional file 1: Materials and Methods. We compared the differentially expressed mRNAs between the control and rotenone-treated groups. The gene expression ratio was expressed as the fluorescence intensity of the rotenone-treated group/fluorescence intensity of the control group. The ratio Log2 (ratio) > 1 was defined as increased genes, and Log2 (ratio) < -1 was defined as decreased genes. Increased or decreased genes only in the Mid glia or Str glia by rotenone treatment were selected using Microarray Data Analysis Tool Ver 3.2 (Filgen, Inc., Aichi, Japan). The gene list is provided in Additional file 4.

#### Protein preparation and western blot analysis

To measure protein levels of nuclear factor-κB (NF-κB) (p65) or nuclear factor of activated T cells 3 (NFATc3), nuclear or cytosol lysates from the cells were extracted and prepared using the NE-PER™ Nuclear and Cytoplasmic Extraction Reagents (Thermo Fisher Scientific,

Waltham, MA) according to the manufacturer's instructions. Mid microglia was treated with Control-ACM, Rotenone-ACM or Rotenone-ACM + SPARC Ab for 48 h. Mid glia or Str glia was treated with vehicle or rotenone (1, 2.5, or 5 nM) for 24 h. To analyze the amount of nuclear Nrf2, nuclear lysates from the cells were extracted using the PARIS protein and RNA isolation system (Ambion, Austin, TX). Mid glia or Str glia was treated with vehicle or rotenone (1, 2.5, or 5 nM) for 6 h. For sample preparation from mice brains, the ventral midbrain or striatal tissue was homogenized in ice-cold RIPA buffer containing protease inhibitor cocktail (Thermo Fisher Scientific). Protein concentrations were determined using the DC protein assay kit (Bio-Rad). Western blot analysis was performed as described previously [33]. The detailed experimental procedures are described in Additional file 1: Materials and Methods.

#### Measurement of mitochondrial reactive oxygen species

To detect ROS production in mitochondria, we used the mitochondrion-selective probe MitoTracker Red CM-H2XRos (Invitrogen), which passively diffuses across the plasma membrane and accumulates in active mitochondria. Mid glia or Str glia was treated with vehicle or rotenone (1, 2.5, or 5 nM) in DMEM-FBS for 6 h, and then incubated with 200 nM MitoTracker Red for 45 min in a $CO_2$ incubator. After incubation, the cells were washed with PBS and observed under a laser microscope. The fluorescence intensity was analyzed using ImageJ software (NIH).

#### Complex I enzyme activity assay

To examine the effect of rotenone treatment on mitochondrial function in Mid glia or Str glia, we measured complex I enzyme activity using the Complex I Enzyme Activity Microplate Assay Kit (ab109721, Abcam, Cambridge, UK), according to the manufacturer's instructions. The detailed experimental procedures are described in Additional file 1: Materials and Methods.

#### ATP assay

To examine whether rotenone treatment produced cytotoxicity in Mid glia or Str glia, we performed an ATP-monitoring luminescence assay using ATPlite Luminescence Assay System (6016943, Perkin Elmer, Akron, OH), according to the manufacturer's instructions. The detailed experimental procedures are described in Additional file 1: Materials and Methods.

#### Determination of glutathione (GSH) content in GCM

GSH content in serum-free GCM was determined using the enzymatic recycling method of Tietze [53] with some modifications [35]. The detailed experimental procedures are described in Additional file 1: Materials and Methods.

#### Enzyme-linked immunosorbent assay (ELISA)

The MT-1 level in serum-free GCM was measured by ELISA with rat MT-1 ELISA kit (SEB119Ra; Cloud-Clone Corp., Houston, TX) according to the manufacturer's instructions. The detailed experimental procedures are described in Additional file 1: Materials and Methods.

#### Statistical analyses

All statistical analyses were performed using KaleidaGraph v5.0 software. Data are presented as dot plots with individual values and bar charts with mean ± SEM. The independent *t* test was used for all comparisons between the two groups. For comparisons between multiple groups, we used one-way ANOVA followed by *post-hoc* Fisher's PLSD test. $p < 0.05$ was considered statistically significant. The complete statistical information is provided in Additional file 5.

## Results

#### Midbrain, but not striatal, glia mediate rotenone-induced dopaminergic neurodegeneration

To examine the effects of regional differences of glial cells on dopaminergic neurotoxicity after rotenone exposure, Mid neuron, Mid neuron + Mid glia, or Mid neuron + Str glia was treated with low-dose rotenone (1, 2.5, or 5 nM) for 48 h (Fig. 1a). Direct exposure of Mid neuron to rotenone (1–5 nM) did not reduce the number of TH-positive dopaminergic neurons. Conversely, TH-positive neurons were significantly decreased by rotenone exposure in the Mid neuron + Mid glia, but not in the Mid neuron + Str glia (Fig. 1b).

To confirm whether rotenone-induced dopaminergic neurotoxicity was mediated by midbrain glial cells, Mid neuron was treated with Mid or Str Rotenone-GCM for 48 h. To exclude the possibility that rotenone reacted with molecules in GCM and damaged dopaminergic neurons, we added rotenone to the GCM directly at the same concentration (GCM + Rotenone) and treated neuronal cultures with the GCM + Rotenone (Fig. 1c). Treatment with Mid Rotenone (5 nM)-GCM shortened the axons and dendrites of dopaminergic neurons and reduced the total number of TH-positive neurons; however, GCM + Rotenone did not (Fig. 1d, e). In contrast, there was no dopaminergic neurotoxicity following treatment with Str Rotenone-GCM (Fig. 1d, e). These data support the results from the cocultured cells shown in Fig. 1b. Our findings indicate that extremely low-dose rotenone cannot induce direct neurotoxicity, but midbrain glia mediate rotenone-induced dopaminergic neurotoxicity.

### Rotenone-exposed midbrain glia increase DA quinone formation in midbrain neurons resulting in dopaminergic neuron-specific neurodegeneration

Next, we examined whether the Mid Rotenone-GCM induced dopaminergic neuron-specific neurotoxicity. The proportions of dopaminergic, GABAergic, and serotonergic neurons were 1%, 46.8%, and 52.2%, respectively, in Mid neuron used in our study (Fig. 2a). We demonstrated morphological changes in GABAergic and serotonergic neurons after Mid Rotenone-GCM treatment via immunohistochemistry using anti-glutamate decarboxylase (GAD) and anti-tryptophan hydroxylase 2 (TPH2) antibodies, respectively (Fig. 2b). Interestingly, Mid Rotenone-GCM did not decrease the number of GAD-positive GABAergic and TPH2-positive serotonergic neurons but rather increased it; these results were completely different from the changes in TH-positive neurons (Fig. 2c).

Next, we examined whether endogenous DA was required for midbrain glia-mediated rotenone-induced dopaminergic neurotoxicity. Mid neuron was treated with the TH inhibitor, AMPT, to deplete intracellular DA, and then co-treated with Mid Rotenone (5 nM)-GCM for 48 h. DA depletion significantly and completely inhibited the Rotenone-GCM-induced dopaminergic neurodegeneration (Fig. 2d). Furthermore, we measured DA quinone formation (quinoprotein), which is a dopaminergic neuron-specific oxidative stress marker formed by autoxidation of intracellular DA, in Mid neuron 48 h after treatment with Mid or Str Control- or Rotenone (5 nM)-GCM. Mid Rotenone-GCM, but not Str Rotenone-GCM, significantly increased quinoprotein levels in neurons (Fig. 2e). These findings suggest that rotenone-exposed midbrain glia increase DA quinone formation in neurons resulting in dopaminergic neuron-specific neurodegeneration.

### Rotenone requires both midbrain astrocytes and microglia to induce dopaminergic neurodegeneration

Mid glia or Str glia contains astrocytes and microglia. To examine whether both astrocytes and microglia are required for rotenone-induced dopaminergic neurotoxicity, we prepared monocultures with > 99.9% microglia or astrocytes from the midbrain and striatum. Mid neuron was treated with Rotenone-MCM from rotenone (5 nM)-treated Mid or Str microglia or Rotenone-ACM from rotenone-treated Mid or Str astrocyte for 48 h as well as Rotenone-GCM (Fig. 3a). Surprisingly, there was no change in the number of TH-positive dopaminergic neurons after treatment with Mid or Str Rotenone-MCM or Rotenone-ACM; in contrast, dopaminergic neuronal death was induced by the Mid Rotenone-GCM (Fig. 3a).

Mid glia contained 87.7% astrocytes and 12.3% microglia; in addition, Str glia contained 98.6% astrocytes and 1.4% microglia (Fig. 3b). Therefore, we explored the possibility that a high number of microglia in Mid glia could lead to rotenone-induced dopaminergic neuronal death. We constructed astrocyte and microglia coculture, in which the content ratio was adjusted to Mid glia or Str glia. Even though the microglial content ratio increased to 12% in the striatal astrocyte and microglia coculture, the Str Rotenone-CM did not reduce the number of TH-positive neurons but rather significantly increased (Fig. 3b). On the other hand, when the content ratio of microglia in the midbrain astrocyte and microglia coculture decreased to 1.2%, the Mid Rotenone-CM failed to induce dopaminergic neurodegeneration (Fig. 3b). These data indicate that midbrain-specific astrocyte-microglia interactions are required for rotenone-induced dopaminergic neurotoxicity.

### Rotenone targets midbrain astrocytes prior to microglia to induce dopaminergic neurodegeneration

To explore whether rotenone targeted astrocytes or microglia, we prepared conditioned media from Mid microglia that were treated with Control-ACM (control-ACM-MCM) or Rotenone (5 nM)-ACM (Rotenone-ACM-MCM) (Fig. 4a); conversely, we prepared conditioned media from Mid astrocyte that were treated with Control-MCM (Control-MCM-ACM) or Rotenone (5 nM)-MCM (Rotenone-MCM-ACM) (Fig. 4b). To exclude the possibility that rotenone reacts with molecules in ACM or MCM and affects microglia or astrocytes, respectively, we added rotenone (5 nM) to the ACM or MCM directly and treated microglia with the rotenone-added ACM (ACM + Rotenone-MCM) (Fig. 4a) or treated astrocytes with the rotenone-added MCM (MCM + Rotenone-ACM) (Fig. 4b). Rotenone-ACM-MCM induced dopaminergic neurotoxicity; however, Rotenone-MCM-ACM did not (Fig. 4). ACM + Rotenone-MCM had no effect on the cell viability of dopamine neurons (Fig. 4a). These findings suggest that rotenone targets midbrain astrocytes prior to microglia to induce dopaminergic neurotoxicity.

### Midbrain astrocytes secrete SPARC by rotenone exposure and induce the toxic conversion of microglia resulting in dopaminergic neurodegeneration

To investigate the molecules secreted from midbrain astrocytes by rotenone exposure, which can act on microglia, we performed secretomic analysis using Mid Control- or Rotenone-ACM (Fig. 5a). Proteins in the concentrated ACM were separated on SDS-PAGE and visualized by silver staining (Fig. 5a). Increased bands in the Rotenone-ACM were sliced and analyzed by LC–MS/MS. The proteins were identified by searching in the NCBI database within *Rattus norvegicus* species and considered on the basis of their molecular weight (Supplementary file 2). We focused on SPARC because

the protein has already been reported to be secreted from astrocytes and to induce immune cell activation [45, 52]. An increase in SPARC in the Mid Rotenone-ACM was confirmed by western blotting (Fig. 5b). We also examined morphological changes in Mid astrocyte after rotenone treatment by immunohistochemistry for glial fibrillary acidic protein (GFAP), an astrocyte marker (Fig. S1a). We did not observe apparent morphological changes by rotenone exposure. GFAP signal density was not changed by rotenone exposure (Fig. S1b).

To examine whether SPARC secreted from rotenone-treated astrocytes induced the toxic conversion of microglia and dopaminergic neurodegeneration, Mid microglia was treated with Control-ACM, Rotenone-ACM or Rotenone-ACM pre-incubated with anti-SPARC Ab (Rotenone-ACM + SPARC Ab), and then each conditioned medium, Control-ACM-MCM, Rotenone-ACM-MCM or Rotenone-ACM + SPARC Ab-MCM was added to Mid neuron (Fig. 5c). Absorption of SPARC in Rotenone-ACM by SPARC Ab significantly prevented Rotenone-ACM-MCM-induced dopaminergic neuronal death (Fig. 5d). Treatment with Rotenone-ACM increased the number of microglia, which was confirmed by immunohistochemistry for the microglial markers Iba1 and CD11b; incubation with SPARC Ab completely inhibited microglial proliferation (Fig. 5e, f). We performed morphological analysis in Mid microglia by measuring area ($\mu m^2$), perimeter (μm), and circularity of Iba1-positive microglia (Fig. S1c and d). Treatment with Rotenone-ACM increased area and perimeter and decreased circularity; incubation with SPARC Ab had no effect (Fig. S1d). Rotenone-ACM also increased the levels of interleukin (IL)-1β and tumor necrosis factor (TNF)-α, which were inhibited by incubation with SPARC Ab (Fig. 5g). In addition, we examined changes in NF-κB (p65) levels and nuclear translocation in Mid microglia. Rotenone-ACM treatment increased NF-κB (p65)-positive signals around and in the nucleus (Fig. 5h and S2a). The NF-κB (p65) signal density was significantly increased by Rotenone-ACM treatment, which was completely inhibited by SPARC Ab incubation (Fig. S2b). Furthermore, protein levels of NF-κB (p65) in the nucleus and cytoplasm were measured by western blot analysis. Rotenone-ACM significantly increased NF-κB (p65) levels not only in the nucleus but also cytoplasm, which were significantly inhibited by SPARC Ab (Fig. 5i, S2c and S2d).

#### Rotenone-exposed midbrain glia secrete NFAT-related inflammatory cytokines

Considering that rotenone-induced dopaminergic neurotoxicity was produced via midbrain astrocyte-microglia crosstalk, we investigated events in glial cells after rotenone exposure using Mid glia or Str glia. First, we examined the morphological changes in astrocytes and microglia 48 h after rotenone exposure. The immunoreactivity of GFAP did not change both in the Mid glia and Str glia after rotenone exposure (Fig. S3a); however, the number of CD11b-positive microglia was significantly increased by rotenone (2.5 and 5 nM) in Mid glia, but not in Str glia (Fig. S3b). Microglial CD11b expression is related to neuroinflammatory processes and is correlated with microglial activation. These data suggest that rotenone exposure alters microglia to a neurotoxic profile.

Rotenone is a well-known inhibitor of mitochondrial complex I; therefore, we examined the effects of rotenone (1, 2.5, or 5 nM) exposure for 6 h on mitochondrial function in Mid glia or Str glia. There was no change in the fluorescence of the mitochondrion-selective probe MitoTracker Red CM-H2XRos in Mid glia following rotenone exposure, but 5 nM rotenone rather increased the fluorescence signal in Str glia (Fig. S3c). Furthermore, we measured complex I enzyme activity in Mid glia or Str glia 48 h after rotenone treatment. Rotenone (1, 2.5, or 5 nM) did not decrease mitochondrial complex I activity in Mid glia, but 5 nM rotenone rather increased the activity in Str glia (Fig. S3d). To examine whether rotenone treatment produced cytotoxicity in glial cells, we measured the ATP content in Mid glia or Str glia 48 h after rotenone exposure. Rotenone (1, 2.5, or 5 nM) treatment did not decrease ATP content both in Mid glia and Str glia, but rather increased in Mid glia (Fig. S3e). These results suggest that the extremely low-dose rotenone (1–5 nM) used in this study did not induce cytotoxicity and mitochondrial dysfunction in midbrain and striatal glial cells.

Next, we sought to identify the key molecules secreted from Mid glia in response to rotenone exposure that caused dopaminergic neurodegeneration. We postulated that there could be two possible mechanisms: the secretion of neurotoxic factors; or the decrease in the levels of neurotrophic or neuroprotective factors. We performed proteomic analysis using Mid or Str Control- or Rotenone (5 nM)-GCM (Fig. S4a). Proteins in the concentrated GCM were separated on SDS-PAGE and visualized by silver staining (Fig. S4b). Increased or decreased bands only in the Mid Rotenone-GCM were sliced and analyzed by LC–MS/MS. The proteins were identified by searching in the NCBI database within *Rattus norvegicus* species and considered on the basis of their molecular weight (Additional file 3). We listed some increased (Fig. S4c) or decreased (Fig. S4d) proteins, which have been reported to be related to neuron-glia interactions or PD pathology. A few inflammation-related molecules were increased in Mid Rotenone-GCM (Fig. S4c). On the other hand, neurotrophic or neuroprotective molecules, including antioxidants, growth factors, anti-inflammatory proteins, chaperones, and protein degradation-related molecules, were decreased in Mid Rotenone-GCM (Fig. S4d).

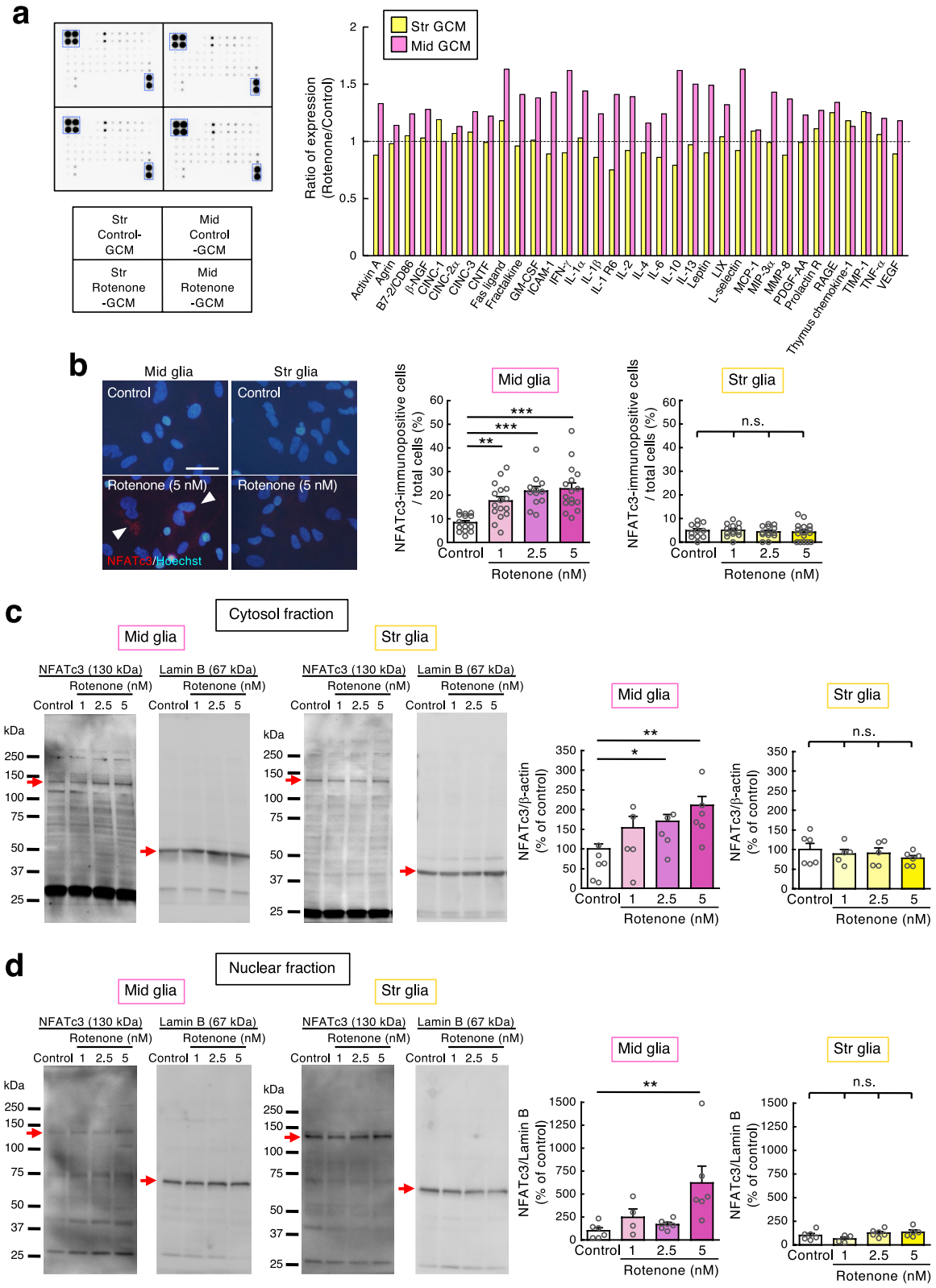


**Fig. 6** (See legend on next page.)

(See figure on previous page.)

**Fig. 6** Rotenone-exposed midbrain glia secrete NFAT-related inflammatory cytokines. **a** Cytokine array analysis using GCM from vehicle- or rotenone (5 nM)-treated Mid glia or Str glia for 48 h. Left, representative images of array membranes. Blue dotted squares represent the positive control. Right, changes in cytokine levels in GCM after rotenone treatment, expressed as ratio of expression (Rotenone/Control). The dotted line shows control levels. **b** NFATc3 immunostaining in Mid glia or Str glia after exposure to rotenone (1, 2.5, or 5 nM) for 15 h. Left, representative images of NFATc3 immunostaining (red) after treatment with Control- or Rotenone (5 nM)-GCM for 15 h. NFATc3-positive signals were indicated by arrowheads. Blue, nuclear staining with Hoechst 33342. Scale bar = 50 µm. Right, quantitation of NFATc3-immunopositive cells, expressed as a percentage of NFATc3-immunopositive cells to total cell number. $^{**}p < 0.01$, $^{***}p < 0.001$ versus control. n.s., not significant. **c, d** Western blot analysis of dephosphorylated NFATc3 (130 kDa) using cytosol (**c**) or nuclear (**d**) fraction of Mid glia or Str glia after treatment with vehicle or rotenone (1, 2.5, or 5 nM) for 24 h. Left, full-length blots; β-action or Lamin B is used as a loading control. Right, quantitation of NFATc3. Each value represents the density of the specific protein signal relative to β-actin or Lamin B, and is presented as a percentage of the control group. $^{*}p < 0.05$, $^{**}p < 0.01$ versus control. n.s., not significant. All data represent mean ± SEM, and are analyzed using one-way ANOVA followed by post-hoc Fisher's PLSD test.

We screened for differentially expressed molecules in GCM from Mid glia or Str glia 48 h after rotenone (5 nM) exposure using a cytokine antibody array. There were small changes in cytokine levels in the Str Rotenone-GCM; in contrast, many inflammatory cytokines were increased in Mid Rotenone-GCM (Fig. 6a). The molecules that were particularly increased in Mid Rotenone-GCM were Fas ligand, granulocyte macrophage-colony stimulating factor (GM-CSF), intercellular adhesion molecule 1 (ICAM-1), interferon (IFN)-γ, IL-1β, IL-1 R6, IL-2, IL-4, IL-6, IL-10, IL-13, and leptin, which are regulated by NFAT [41, 51, 57]. L-Selectin, which activates NFAT signaling, was also upregulated in Mid Rotenone-GCM (Fig. 6a). We also performed cDNA microarray to search for genes whose expression was upregulated or downregulated only in the Mid glia after rotenone treatment (5 nM) for 24 h. NFATc3 was significantly upregulated in Mid glia by rotenone exposure (Additional file 4). Therefore, we examined the effects of rotenone on NFATc3 in Mid glia or Str glia. Immunostaining revealed an increase in NFATc3-positive cells in the Mid glia, but not Str glia, after rotenone treatment for 15 h and 24 h (Fig. 6b and Fig. S5). The NFATc3-positive signals were observed mainly around nucleus (Fig. 6b). Therefore, we measured NFATc3 protein levels in the cytoplasm of Mid glia or Str glia after rotenone treatment for 24 h by western blot analysis. Rotenone (2.5 and 5 nM) significantly increased the level of dephosphorylated NFATc3 (130 kDa), which is the activated form, in the cytoplasm of Mid glia (Fig. 6c). Furthermore, we confirmed the nuclear translocation of NFATc3 by western blot analysis of the nuclear fraction of Mid glia or Str glia 24 h after rotenone exposure. Rotenone (5 nM) significantly increased the dephosphorylated NFATc3 levels in the nuclei of Mid glia (Fig. 6d). In contrast, rotenone treatment did not affect NFATc3 levels both in the cytoplasm and nuclei of Str glia (Fig. 6c, d). These data were consistent with the results showing the rotenone-induced release of inflammatory cytokines from Mid glia (Fig. 6a). These findings indicate that rotenone activates the NFAT signaling pathway in midbrain glia to stimulate the release of inflammatory cytokines into the extracellular space.

### Reduced secretion of the antioxidant MT from midbrain glia by rotenone exposure contributes to dopaminergic neurotoxicity

Compared with other neurons, dopaminergic neurons are especially vulnerable to oxidative stress because dopaminergic neurons contain DA, which can produce ROS and DA quinone [4, 30]. Therefore, a reduction in antioxidants may be particularly detrimental to dopaminergic neurons. The synthesis of GSH, a well-known antioxidant, in neurons depends on the release of GSH from astrocytes into the extracellular space [55]. In addition, GSH scavenges DA quinones directly [17]. MTs are cysteine-rich metal-binding proteins [6]. MT-1, a major isoform, possesses antioxidative properties by scavenging free radicals and exerts anti-inflammatory effects by suppressing microglial activation in the brain [6, 40]. We previously reported that MT-1 quenched DA semiquinones in vitro [31] and that the protein was upregulated specifically in astrocytes in response to oxidative stress to protect dopaminergic neurons against DA quinone toxicity [32]. In this study, we examined the possibility that neuroprotective molecules secreted from midbrain glial cells, mainly astrocytes, were decreased following rotenone exposure. As shown in Fig. 2e, DA quinone formation was increased by treatment with Mid Rotenone-GCM. Therefore, we measured the GSH and MT-1 levels in GCM from Mid glia or Str glia after rotenone treatment for 48 h. Rotenone did not affect the GSH content in the GCM from both Mid glia and Str glia (Fig. S6a). MT-1 was significantly reduced in the GCM from Mid glia, but not Str glia, following rotenone (1–5 nM) treatment (Fig. 7a). Nuclear factor erythroid 2-related factor 2 (Nrf2) regulates the expression of various GSH-related molecules, such as γ-glutamyl cysteine ligase and GSH synthetase [48]. Our previous studies demonstrated that MT-1 expression was regulated by Nrf2 [32, 33]. Therefore, we examined the effects of rotenone treatment on the protein levels of Nrf2 in the nuclei of midbrain and striatal glial cells. There was no change in nuclear Nrf2 levels following 6 h of rotenone exposure (Fig. S6b). These results suggest that rotenone inhibits MT-1 release from Mid glia but not Nrf2-mediated synthesis.

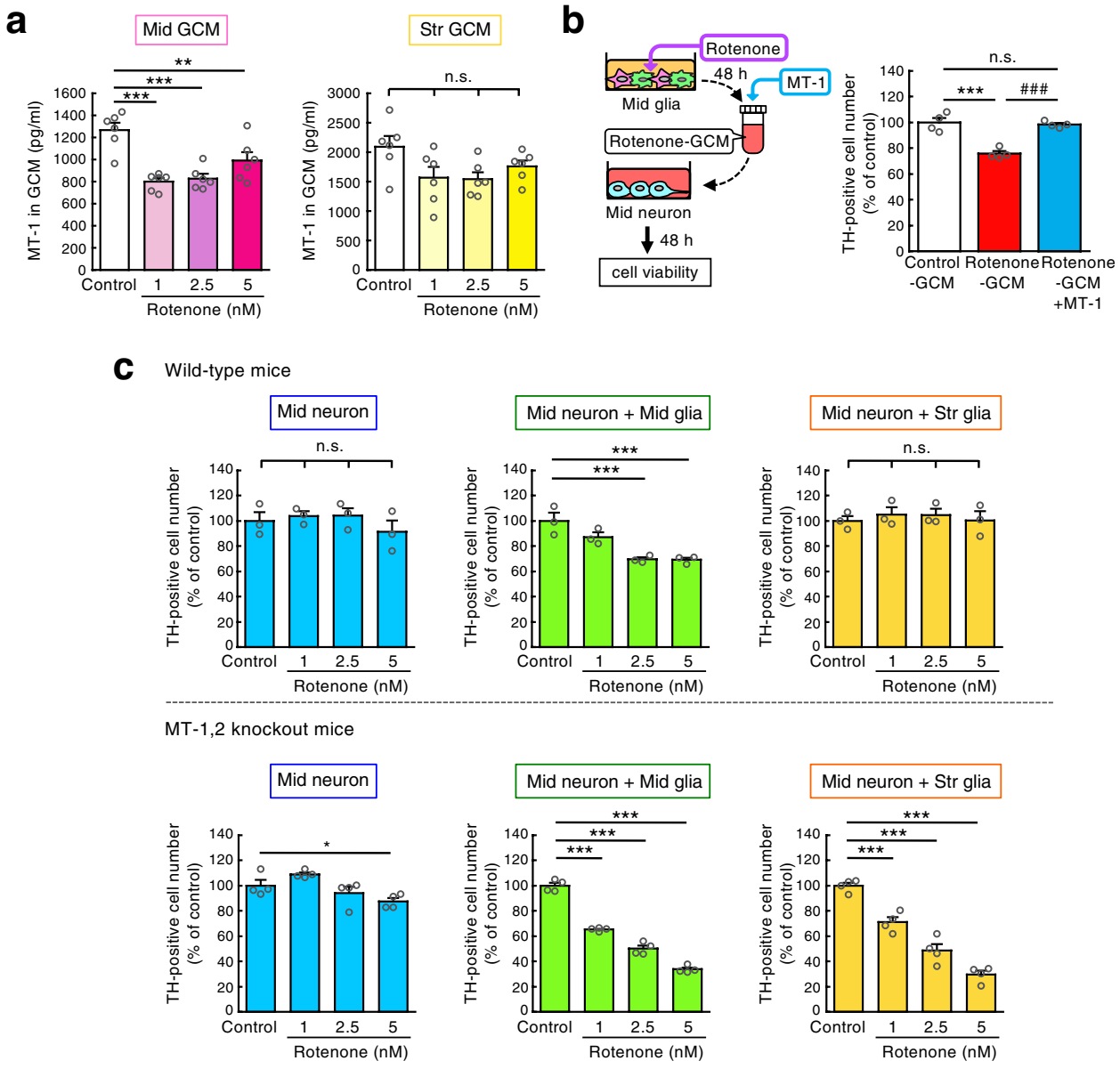


**Fig. 7** Reduction in the secretion of the antioxidant MT from midbrain glia by rotenone exposure contributes to dopaminergic neurotoxicity. **a** Measurement of MT-1 content in Control- or Rotenone-GCM from Mid glia or Str glia after treatment with vehicle or rotenone (1, 2.5, or 5 nM) for 48 h. $^{**}p < 0.01$, $^{***}p < 0.001$ versus control. n.s., not significant. **b** Supplementation of MT-1 to Mid Rotenone-GCM inhibited dopaminergic neurotoxicity. Left, schematic illustration of cell treatment. The Mid neuron was treated with GCM from vehicle- or rotenone (5 nM)-treated Mid glia with/without MT-1 recombinant protein (300 pg/ml) for 48 h. Right, number of TH-positive neurons, expressed as a percentage of the control. $^{***}p < 0.001$ versus Control-GCM, $^{\#\#\#}p < 0.001$ versus Rotenone-GCM. n.s., not significant. **c** Lack of MT-1,2 induced dopaminergic neurodegeneration mediated by rotenone-treated Str glia as well as Mid glia. Cell viability analysis of dopaminergic neurons after treatment with vehicle or rotenone (1, 2.5, or 5 nM) for 24 h in the Mid neuron, Mid neuron + Mid glia, or Mid neuron + Str glia of wild-type mice (top) or MT-1,2 knockout mice (bottom), expressed as a percentage of the control. $^{*}p < 0.05$, $^{***}p < 0.001$ versus control. n.s., not significant. All data represent mean ± SEM, and are analyzed using one-way ANOVA followed by *post-hoc* Fisher's PLSD test.

Next, we examined whether the reduction in MT-1 secretion from Mid glia by rotenone exposure could promote dopaminergic neurodegeneration. Rotenone (5 nM) exposure reduced MT-1 in Mid GCM by 300 pg/ml (Fig. 7a). Therefore, Mid neuron was treated with Mid Rotenone (5 nM)-GCM with/without MT-1 recombinant protein (300 pg/ml) for 48 h (Fig. 7b). Supplementation of MT-1 to Mid Rotenone-GCM completely rescued dopamine neurons from rotenone toxicity (Fig. 7b). The MT family comprises four isoforms: MT-1, MT-2, MT-3, and MT-4. The MT-1 and MT-2 isoforms share very high sequence homology and have similar expression profiles and functions; therefore, they are usually considered as a single isoform (denoted MT-1,2 in this

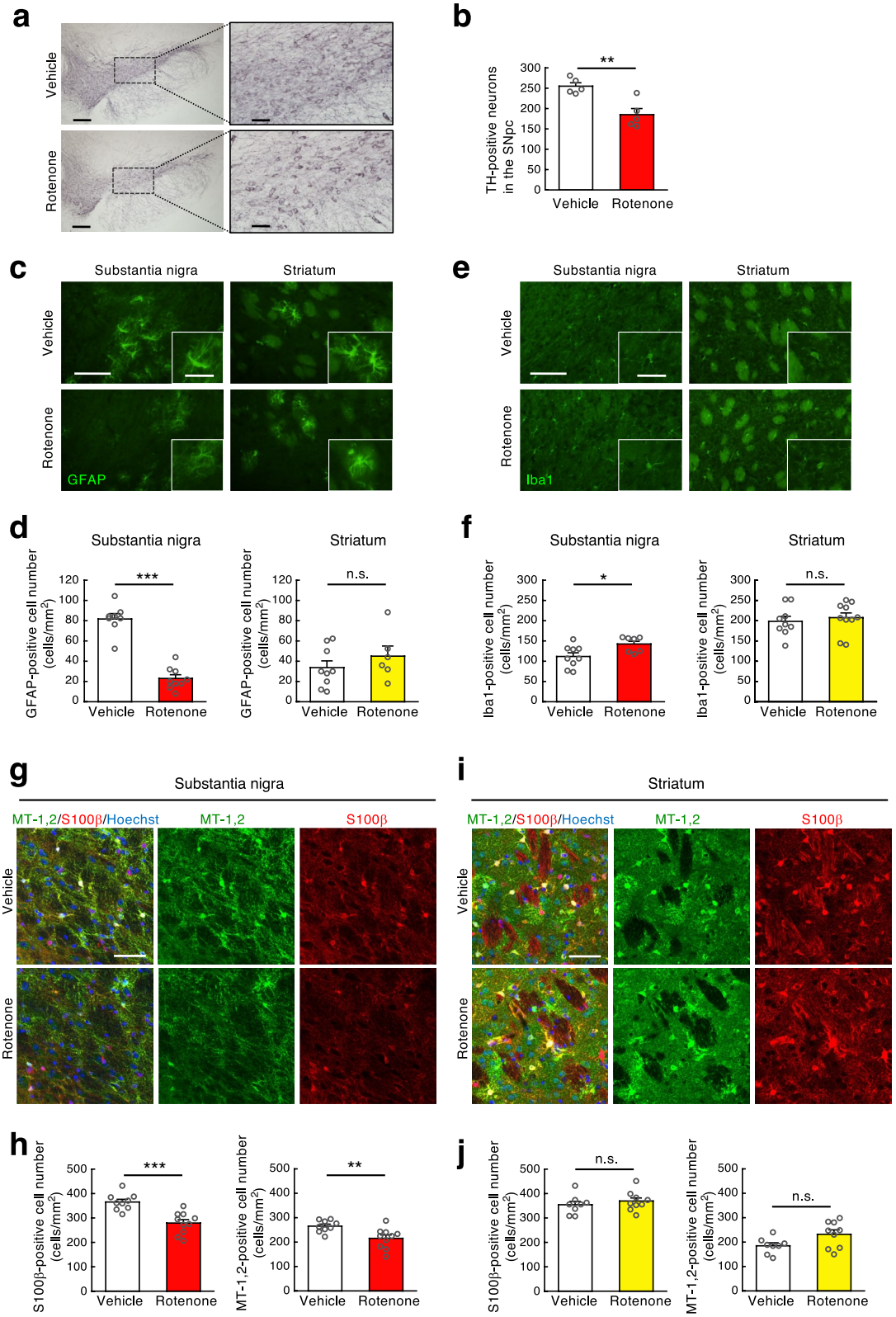


**Fig. 8** (See legend on next page.)

(See figure on previous page.)

**Fig. 8** Glial response in the SNpc and striatum of low-dose rotenone-injected PD model mice. **a** Representative images of TH immunostaining in the SNpc of vehicle- or rotenone (2.5 mg/kg/day)-injected mice at two different magnifications. The right panels are high-magnification images of the left panels (squared areas). Scale bar = 200 μm (left) or 50 μm (right). **b** Cell number of TH-positive neurons in the SNpc. $^{**}p < 0.01$ versus vehicle-injected control group. **c-f** Regional differences in the response of astrocytes and microglia to rotenone treatment. **c**, **e** Representative images of GFAP (**c**) or Iba-1 (**e**) immunostaining in the SNpc and striatum of vehicle- or rotenone-injected mice. Scale bar = 50 μm. Insets show higher magnification images of astrocytes or microglia. Scale bar = 10 μm. **d**, **f** Number of GFAP (**d**) or Iba-1 (**f**) positive cells in the SNpc or striatum. $^{*}p < 0.05$, $^{***}p < 0.001$ versus vehicle-injected control group. n.s., not significant. **g-j** Regional differences in MT-1,2-expressing astrocytes after rotenone treatment. **g, i** Representative images of MT-1,2 and S100β immunostaining in the SNpc (**g**) and striatum (**i**) of vehicle- or rotenone-injected mice. Green, MT-1,2. Red, S100β-positive astrocytes. Scale bar = 50 μm. **h**, **j** Number of S100β- or MT-1,2-positive cells in the SNpc (**h**) or striatum (**j**). $^{**}p < 0.01$, $^{***}p < 0.001$ versus vehicle-injected control group. n.s., not significant. All data represent mean ± SEM, and are analyzed using independent *t* test

study). We prepared Mid neuron, Mid neuron + Mid glia, and Mid neuron + Str glia using the mesencephalon and striatum of embryos from MT-1,2 knockout or wild-type mice. Cultured cells were treated with rotenone (1, 2.5, or 5 nM) for 24 h, after which the number of TH-positive neurons was counted. We detected a reduction in the number of TH-positive neurons following rotenone treatment in the Mid neuron + Mid glia from wild-type mice, but no difference in the Mid neuron or Mid neuron + Str glia (Fig. 7c), which coincided with our rat primary cultured cell data (Fig. 1b). Conversely, in cultured cells from MT-1,2 knockout mice, the number of TH-positive cells was significantly decreased by rotenone exposure not only in the Mid neuron + Mid glia but also in the Mid neuron and Mid neuron + Str glia (Fig. 7c). These findings indicate that MT-1,2 are important molecules that can be targeted for the inhibition of rotenone-induced dopaminergic neurodegeneration. Furthermore, these data strongly support the hypothesis that the loss of antioxidant properties in glia, mainly astrocytes, produces rotenone-induced dopaminergic neurodegeneration.

### Increase in microglia and reduction in MT-expressing astrocytes in the SNpc, but not in the striatum, of low-dose rotenone-injected PD model mice

We explored regional differences in the glial response in animal models of PD produced by chronic systemic exposure to low-dose rotenone (2.5 mg/kg/day) for 4 weeks by subcutaneous implantation of rotenone-filled osmotic mini pump; the rotenone-treated mice reproduced the behavioral and central and peripheral neurodegenerative features of PD [34]. Rotenone treatment significantly decreased the number of TH-positive dopaminergic neuronal cells in the SNpc (Fig. 8a, b). We further examined the morphological changes in astrocytes and microglia in the SNpc and striatum of rotenone-injected mice by immunostaining for GFAP and Iba1. The number of GFAP-positive astrocytes was significantly decreased in the SNpc but not in the striatum (Fig. 8c, d). In addition, the number of Iba1-positive microglia was significantly increased in the SNpc but not in the striatum (Fig. 8e, f). Next, we measured protein levels of SPARC in the ventral midbrain and striatum of rotenone-injected mice by western blot analysis. SPARC was increased in the ventral midbrain, but not in the striatum (Fig. S7a). Next, we examined changes in IL-1β and TNF-α in the ventral midbrain by western blot analysis. The levels of IL-1β and TNF-α tended to increase by rotenone injection, although those were not significant (Fig. S7b and S7c). Furthermore, we examined the effects of rotenone exposure on MT-1,2 expression in astrocytes in the SNpc and striatum. To assess MT-1,2 expression in all types of astrocytes, including protoplasmic astrocytes, we chose an anti-S100β Ab as the astrocyte marker. The number of S100β- and MT-1,2-positive astrocytes was significantly decreased in the SNpc but not in the striatum (Fig. 8g–j), which is consistent with the results of the cell culture experiments (Fig. 7a).

## Discussion

The present study revealed that low-dose rotenone cannot induce neurotoxicity via direct exposure on neurons, but midbrain-specific astrocyte-microglia crosstalk produces rotenone-induced dopaminergic neurodegeneration. Under normal conditions, astrocytes support and protect neurons by supplying their energy source, producing antioxidants and neurotrophic factors, and removing potentially neurotoxic molecules, such as excess glutamate, in the synaptic space [32, 37, 42, 49]. In addition, microglia maintain neuronal function by the removal of neuronal debris and protein aggregates [23]. Therefore, we hypothesized that glial cells protect dopaminergic neurons against rotenone neurotoxicity. However, we found that midbrain glia promoted rotenone-induced dopaminergic neurodegeneration. Interestingly, striatal glia had no effect on rotenone neurotoxicity.

The mechanism of selective dopaminergic neurodegeneration induced by rotenone has yet to be elucidated. Inhibition of complex I followed by ATP depletion cannot fully explain the selectivity of dopaminergic neuronal damage, and oxidative stress is considered to be involved [10, 47]. Some studies have demonstrated that ROS are produced via the inhibition of mitochondrial complex I by rotenone [38, 47]. It has been suggested that dopaminergic neurons are vulnerable to mitochondrial defects or oxidative damage. In this study, we showed that rotenone altered the function of midbrain, but not striatal,

glial cells to a neurotoxic profile without affecting mitochondrial complex I activity, which produced selective dopaminergic neuronal death. In addition, we focused on endogenous DA and DA oxidation as primary factors of dopaminergic neuron vulnerability to rotenone. DA is stable in synaptic vesicles under normal physiological conditions; however, cytosolic-free DA is metabolized by monoamine oxidase, followed by $H_2O_2$ production. In dopaminergic neurons, where transition metals are abundant, $H_2O_2$ can react with metals, especially iron, to form the most cytotoxic hydroxyl radical. In addition, cytosolic DA is spontaneously oxidized and produces $O_2^-$ and reactive DA quinones [4]. DA quinones exert cytotoxicity by binding with the sulfhydryl groups of various bioactive molecules, such as the TH and DA transporters, to form quinoproteins and inactivate these molecules [24, 26, 56]. We previously demonstrated that DA quinone is involved in dopaminergic neurotoxicity in PD models [3, 4]. In this study, we demonstrated that intracellular DA depletion by a TH inhibitor completely inhibited the dopaminergic neurotoxicity induced by exposure to GCM from rotenone-treated Mid glia. These data are in line with previous studies that showed the involvement of DA in rotenone-induced dopaminergic neuronal death [2, 46]. Furthermore, treatment with Mid Rotenone-GCM increased quinoprotein levels. The quinone formation is closely linked to general oxidative stress, mitochondrial dysfunction, inflammation, and proteasome impairment [9, 25, 30, 58]. These findings suggest that dopaminergic neurons are intrinsically sensitive to rotenone because of the presence of intracellular DA and the resulting oxidative stress. Furthermore, dysfunction of midbrain glia would disclose the vulnerability of dopaminergic neurons.

Here, we demonstrated that Rotenone-MCM from Mid microglia or Rotenone-ACM from Mid astrocyte did not affect dopamine neurons; in contrast, Rotenone-GCM from Mid glia (astrocyte + microglia) induced dopaminergic neurodegeneration. These results indicate that rotenone requires midbrain astrocyte-microglia interactions to induce dopaminergic neurotoxicity. In our experiments, Mid glia or Str glia contained 12.3% microglia and 87.7% astrocytes or 1.4% microglia and 98.6% astrocytes, respectively; thus, there were approximately ten times more microglia in the Mid glia than that in the Str glia. This might raise a possibility that differences in the dopaminergic neurotoxicity of Mid and Str Rotenone-GCM could be simply due to differences in the proportions of astrocytes and microglia. Therefore, we constructed astrocyte and microglial cocultures, in which the content ratio was adjusted to Mid glia or Str glia. Even though the microglial population in the striatal astrocyte and microglial cocultures increased to 12% to adjust to that of Mid glia, the Rotenone-CM did not cause dopaminergic neurotoxicity. When the content ratio of microglia in midbrain astrocyte and microglia cocultures decreased to 1.2%, the Rotenone-CM failed to induce dopaminergic neurodegeneration. We conjecture that neurotoxic effects might be undetectable due to the low content of microglia. These data indicate that rotenone-induced dopaminergic neurotoxicity is dependent on a brain region-specific glial response to rotenone exposure. Various reports, including our previous studies of the regional heterogeneity of glia, support this hypothesis. We demonstrated that MT-1,2 were upregulated in reactive astrocytes specifically in the striatum, but not in the cortex, in methamphetamine-injected mice with dopaminergic nerve terminal degeneration [32]. In addition, the administration of a serotonin 1A agonist induced astrocyte proliferation and upregulated astrocytic MT expression in the striatum but not in the SN of mice [33]. Furthermore, neurotoxin 6-OHDA treatment upregulated Nrf2-regulating antioxidative molecules in striatal, but not mesencephalic, astrocytes [5]. These findings in our previous studies suggest regional differences, especially in astrocytic responses to different stimuli, and that striatal astrocytes are more reactive than midbrain (mesencephalic) astrocytes. Like astrocytes, the regional heterogeneity of microglia has also been recognized [15]. The midbrain-specific microglia show an immune-alerted phenotype, such as an increase in inflammatory markers [1, 54]. It has been reported that midbrain microglia highly express major histocompatibility complex class II and toll-like receptor 4 than microglia in the cortex, hippocampus, and striatum under basal conditions [1]. The transcriptome profiles of microglia in the midbrain are similar to those of inflammation-associated microglia [54]. These findings suggest that regional differences in astrocytes and microglia can contribute to region-specific neuronal vulnerability.

Activated microglia are known to convert astrocytes to neurotoxic A1 astrocytes; A1 astrocytes upregulate pro-inflammatory factors, such as IL-1α, IL-1β, and TNF-α, lose the ability to promote neuronal survival, outgrowth, and phagocytosis, and induce neuronal death [27]. Conversely, astrocytes control microglial activation and microglia-induced neuroinflammation [44]. Here, we demonstrated that Rotenone-ACM-MCM induced dopaminergic neurotoxicity; however, Rotenone-MCM-ACM did not. These results indicate that rotenone targeted midbrain astrocytes prior to microglia in dopaminergic neurodegeneration. As shown in Fig. 3, Rotenone-ACM did not induce dopaminergic neuronal death. Taken together, these results suggest that rotenone-exposed astrocytes induce neurotoxic conversion of microglia. To identify molecules secreted from midbrain astrocytes by rotenone exposure that can act on microglia, we performed secretomics using Control- or Rotenone-ACM

from Mid astrocyte, and identified SPARC as a mediator from astrocytes to microglia. SPARC, a matricellular protein, is known to be upregulated by reactive astrocytes and influences immune cell activation [45, 52]. Recent studies have demonstrated that SPARC converts anti-inflammatory macrophages into a proinflammatory phenotype [45]. In this study, Rotenone-ACM induced microglial proliferation, increase in IL-1β and TNF-α, and NF-κB (p65) nuclear translocation in microglia; these effects were completely inhibited by incubation with SPARC Ab. Furthermore, the absorption of SPARC in Rotenone-ACM by SPARC Ab significantly prevented Rotenone-ACM-MCM-induced dopaminergic neuronal death. Taken together, these findings suggest that midbrain astrocytes secrete SPARC by rotenone exposure and induce the toxic conversion of microglia resulting in dopaminergic neurodegeneration. In this study, we collected conditioned media by one-way transfer of cultured media, i.e., astrocyte-to-microglia or microglia-to-astrocyte; however, it is possible that microglia influenced by rotenone-exposed astrocytes may further act on astrocytes to convert them to neurotoxicity. Therefore, bidirectional astrocyte-microglia interactions could contribute to rotenone neurotoxicity. Furthermore, we examined morphological changes in Mid astrocyte after rotenone exposure and Mid microglia after treatment with Control-ACM, Rotenone-ACM or Rotenone-ACM + SPARC Ab. It is known that increase in GFAP immunoreactivity indicates morphological activation of astrocytes. In Mid astrocyte, GFAP signal density did not change with rotenone exposure, suggesting that morphological activation of astrocytes did not occur by rotenone treatment. In Mid microglia, area and perimeter of Iba1-positive microglia were increased after treatment with Rotenone-ACM, suggesting microglial activation; however, SPARC Ab did not inhibit the microglial activation. These results suggest that morphological and functional changes in astrocytes or microglia do not necessarily coincide.

In this study, we sought to identify key molecules present in the GCM from Mid glia in response to rotenone exposure that promote dopaminergic neurodegeneration. To verify brain region-specific glial reactivity, molecular changes in GCM from Mid glia or Str glia were assessed in this study. Secretomics identified inflammation-related molecules as increased proteins and antioxidants, growth factors, anti-inflammatory proteins, chaperones, and protein degradation-related molecules as decreased proteins, which were changed in Rotenone-GCM from Mid glia but not Str glia. In addition, we detected an increase in NFAT-related inflammatory cytokines and a decrease in the antioxidant molecule MT-1 in Mid Rotenone-GCM. Indeed, CD11b-positive inflammation-related microglia were increased in Mid glia after rotenone exposure. MT-1,2 are expressed mainly in astrocytes and secreted from the cells [14, 40], and astrocyte-derived MTs can translocate to neurons [13]. MT scavenges free radicals and DA quinone [31]. Our previous study showed that MT-1,2 secreted into the extracellular space from astrocytes protects dopaminergic neurons against oxidative stress [32, 33]. Therefore, reducing MT secretion from astrocytes into the extracellular space may significantly impact dopaminergic neuronal survival due to their vulnerability to oxidative stress. The present study confirmed the contribution of MTs to glia-mediated rotenone toxicity by supplementing recombinant MT-1 to Mid Rotenone-GCM or by using primary cultured cells from wild-type and MT-1,2 knockout mice.

Finally, we examined regional differences in the glial response in PD model mice produced by treatment with a lower dose of rotenone (2.5 mg/kg/day) compared with previous reports [34]. The rotenone-treated mice reproduced the behavioral and central and peripheral neurodegenerative features of PD; the mice exhibited motor deficits, gastrointestinal dysfunction, and neurodegeneration accompanied by accumulation of intracellular α-synuclein in nigrostriatal dopaminergic neurons, cholinergic neurons in the dorsal motor nucleus of the vagus and the intestinal myenteric plexus [34]. However, mitochondrial complex I activity was not reduced in these tissues [34]. This study demonstrated that the number of GFAP-, S100β- and MT-1,2-positive astrocytes was significantly decreased in the SNpc, but not in the striatum; in addition, the number of microglia in the SNpc was increased. Furthermore, SPARC levels were increased in the midbrain, but not in the striatum, of rotenone-injected mice. These data were consistent with the results of cell culture experiments. However, IL-1β and TNF-α did not significantly increase in the midbrain of PD model mice, although microglial proliferation was observed. We examined the amounts of these proteins in tissues in the chronic phase at 4 weeks after rotenone administration, so the period during which the molecular events observed in the culture experiments may have passed. Future studies at earlier time points after the administration will be necessary. Previous studies demonstrated the contribution of glial dysfunction to neurodegeneration in parkinsonian models [36, 50]. Solano et al. reported that lack of a ubiquitin E3 ligase protein parkin, which is one of the genes responsible for early-onset autosomal recessive PD, produced abnormal functions of astrocytes leading to vulnerability of dopaminergic neurons to oxidative stress [50]. In addition, several reports have demonstrated that deficiency of astrocytic DJ-1, whose mutations are also linked to autosomal recessive PD, enhances rotenone-induced neurotoxicity [36]. Moreover, inflammasome activation in microglia promotes neuroinflammation and dopaminergic

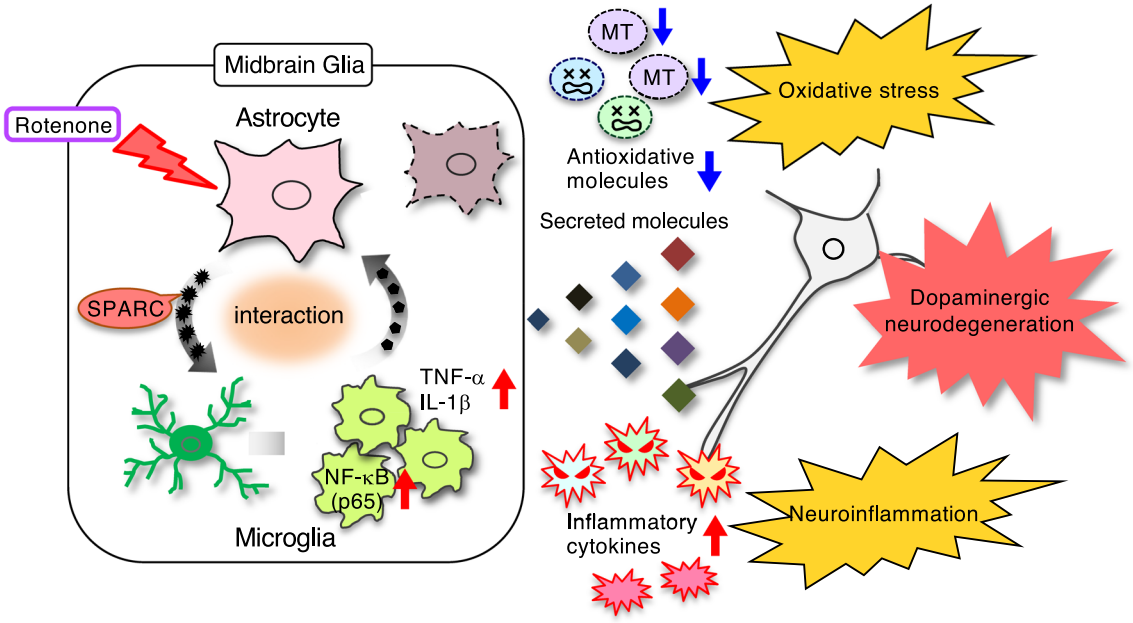


**Fig. 9** Schematic illustration of the possible mechanism of midbrain glia-mediated rotenone-induced dopaminergic neurodegeneration. Rotenone targets midbrain astrocytes, which secrete SPARC and increase NF-κB (p65), TNF-α and IL-1β in microglia. The midbrain-specific astrocyte-microglia interactions induce the release of inflammatory cytokines and a reduction in neuroprotective antioxidants, resulting in dopaminergic neuron-specific neurodegeneration

neurodegeneration [7, 18]. Taken together, our findings in this study suggest that rotenone causes brain region-specific glial dysfunction, such as inflammatory response and reduction in the antioxidative and neuroprotective properties of midbrain (nigral) glia, producing dopaminergic neurodegeneration.

## Conclusions

Our results demonstrated that rotenone targeted midbrain astrocytes and produced glial dysfunction-mediated dopaminergic neurodegeneration. Rotenone-treated midbrain astrocytes secreted SPARC and induced the toxic conversion of microglia. The midbrain-specific astrocyte-microglia interactions induced the release of inflammatory cytokines and a reduction in neuroprotective antioxidants, resulting in dopaminergic neuron-specific neurodegeneration (Fig. 9). Our findings elucidated the mechanism underlying selective dopaminergic neurodegeneration induced by rotenone. Moreover, this study underscores the importance of recognizing the brain region-specific glial crosstalk as a crucial promoter in neurodegenerative diseases.

### Abbreviations

| | |
|---|---|
| PD | Parkinson's disease |
| SPARC | Secreted protein acidic and rich in cysteine |
| MT | Metallothionein |
| ROS | Reactive oxygen species |
| CNS | Central nervous system |
| SNpc | Substantia nigra pars compacta |
| SD | Sprague–Dawley |
| DMEM | Dulbecco's modified Eagle's medium |
| FBS | Fetal bovine serum |
| Ara-C | Cytosine-β-D-arabinofuranoside |
| Mid | Midbrain |
| Str | Striatum |
| DMSO | Dimethylsulfoxide |
| GCM | Glial conditioned medium |
| ACM | Astrocyte conditioned medium |
| MCM | Microglial conditioned medium |
| CM | Conditioned medium |
| Ab | Antibody |
| DA | Dopamine |
| TH | Tyrosine hydroxylase |
| AMPT | α-Methyl-*p*-tyrosine |
| PMSF | Phenylmethylsulfonyl fluoride |
| NF-κB | Nuclear factor-κB |
| NFATc3 | Nuclear factor of activated T cells 3 |
| GSH | Glutathione |
| ELISA | Enzyme-linked immunosorbent assay |
| GAD | Glutamate decarboxylase |
| TPH2 | Tryptophan hydroxylase 2 |
| GFAP | Glial fibrillary acidic protein |
| IL | Interleukin |
| TNF-α | Tumor necrosis factor-α |
| GM-CSF | Granulocyte macrophage-colony stimulating factor |
| ICAM-1 | Intercellular adhesion molecule 1 |
| IFN-γ | Interferon-γ |
| Nrf2 | Nuclear factor erythroid 2-related factor 2 |

## Supplementary Information

The online version contains supplementary material available at https://doi.org/10.1186/s40478-025-02160-3.

Additional file 1: Materials and Methods. Supplementary Table 1. List of antibodies used in this study. Figure S1. Morphological analysis of rotenone-treated Mid astrocyte or Mid microglia after treatment with Control-ACM, Rotenone-ACM or Rotenone-ACM+SPARC Ab. Figure S2. Changes in NF-kB

(p65) levels in Mid microglia after treatment with Control-ACM, Rotenone-ACM or Rotenone-ACM+SPARC Ab. Figure S3. Effects of rotenone exposure on morphological changes and mitochondrial function in Mid glia or Str glia. Figure S4. Secretomics of Rotenone-GCM from rotenone (5 nM)-treated Mid glia. Figure S5. Effects of rotenone exposure for 6, 15, or 24 h on NFATc3-immunopositive cells in Mid glia or Str glia. Figure S6. Effects of rotenone exposure on antioxidative properties in Mid glia or Str glia. Figure S7. Changes in levels of SPARC, IL-1β and TNF-α in the midbrain or striatum of rotenone-injected parkinsonian mice.

Additional file 2: List of proteins in Rotenone-ACM from rotenone (5 nM)-treated Mid astrocyte identified by LC-MS/MS analysis followed by NCBI database.

Additional file 3: List of proteins in Rotenone-GCM from rotenone (5 nM)-treated Mid glia identified by LC-MS/MS analysis followed by NCBI database.

Additional file 4: List of genes whose expression was upregulated or downregulated after rotenone treatment (5 nM) for 24 h in Mid glia or Str glia analyzed by cDNA microarray.

Additional file 5: Complete statistical information.

**Acknowledgements**
We thank Dr. Youichirou Higashi at Kochi University for expert technical support with microglial culture. This work was supported by JSPS KAKENHI Grant for Scientific Research (C) (JP22590934, JP25461279, JP16K09673, JP19K07993 to I.M.), MEXT KAKENHI Grant for Scientific Research on Innovative Areas "Brain Environment" (JP24111533 to M.A.), the Okayama Medical Foundation (to I.M.), and The Sanyo Broadcasting Foundation (to I.M.).

**Author contributions**
I.M. designed and conducted the experiments, analyzed and interpreted the data and wrote the manuscript. N.I. and R.K. assisted with some of the in vitro experiments. N.I., R.K., F.I., K.M. and K.T. assisted with the in vivo experiments. M.S. assisted with proteomic analysis. C.S. and N.S. assisted with experiments using MT-1,2 knockout and wild-type mice. Y.K. reviewed and edited the manuscript. M.A. designed the experiments, interpreted the data and edited the manuscript. All authors discussed the results and commented on the manuscript.

**Funding**
This work was supported by JSPS KAKENHI Grant for Scientific Research (C) (JP22590934, JP25461279, JP16K09673, JP19K07993 to I.M.), MEXT KAKENHI Grant for Scientific Research on Innovative Areas "Brain Environment" (JP24111533 to M.A.), the Okayama Medical Foundation (to I.M.), and The Sanyo Broadcasting Foundation (to I.M.).

**Data availability**
All data generated or analyzed during this study are included in this published article and its supplementary information files.

## Declarations

**Ethics approval and consent to participate**
All experimental procedures were conducted in accordance with the NIH Guide for the Care and Use of Experimental Animals and the Policy on the Care and Use of the Laboratory Animals, Okayama University, and were approved by the Animal Care and Use Committee, Okayama University (approval reference numbers: OKU-2017058, OKU-2017059, OKU-2020004, OKU-2020005, OKU-2023032, and OKU-2023033).

**Consent for publication**
Not applicable.

**Competing interests**
The authors declare no competing interests.

**Author details**
[1]Department of Medical Neurobiology, Okayama University Graduate School of Medicine, Dentistry and Pharmaceutical Sciences, 2-5-1 Shikata-cho, Kita-ku, Okayama 700-8558, Japan
[2]Department of Pharmacy, Okayama University Hospital, Okayama, Japan
[3]Department of Cell Biology, Okayama University Graduate School of Medicine, Dentistry and Pharmaceutical Sciences, Okayama, Japan
[4]Department of Food and Health Sciences, Faculty of Environmental Studies, Hiroshima Institute of Technology, Hiroshima, Japan
[5]Department of Molecular Engineering and Drug Developmental Sciences, Graduate School of Oral Medicine, Matsumoto Dental University, Shiojiri, Japan
[6]Department of Pharmacotherapy, School of Pharmacy, Shujitsu University, Okayama, Japan

Received: 27 February 2025 / Accepted: 14 October 2025
Published online: 14 November 2025

**References**

1. Abellanas MA, Zamarbide M, Basurco L, Luquin E, Garcia-Granero M, Clavero P et al (2019) Midbrain microglia mediate a specific immunosuppressive response under inflammatory conditions. J Neuroinflammation 16:233. https://doi.org/10.1186/s12974-019-1628-8
2. Ahmadi FA, Grammatopoulos TN, Poczobutt AM, Jones SM, Snell LD, Das M et al (2008) Dopamine selectively sensitizes dopaminergic neurons to rotenone-induced apoptosis. Neurochem Res 33:886–901. https://doi.org/10.1007/s11064-007-9532-5
3. Asanuma M, Miyazaki I, Diaz-Corrales FJ, Kimoto N, Kikkawa Y, Takeshima M et al (2010) Neuroprotective effects of zonisamide target astrocyte. Ann Neurol 67:239–249. https://doi.org/10.1002/ana.21885
4. Asanuma M, Miyazaki I, Ogawa N (2003) Dopamine- or L-DOPA-induced neurotoxicity: the role of dopamine quinone formation and tyrosinase in a model of Parkinson's disease. Neurotox Res 5:165–176. https://doi.org/10.1007/BF03033137
5. Asanuma M, Okumura-Torigoe N, Miyazaki I, Murakami S, Kitamura Y, Sendo T (2019) Region-specific neuroprotective features of astrocytes against oxidative stress induced by 6-hydroxydopamine. Int J Mol Sci 20:598. https://doi.org/10.3390/ijms20030598
6. Aschner M (1998) Metallothionein (MT) isoforms in the central nervous system (CNS): regional and cell-specific distribution and potential functions as an antioxidant. Neurotoxicology 19:653–660
7. Badanjak K, Fixemer S, Smajic S, Skupin A, Grunewald A (2021) The contribution of microglia to neuroinflammation in Parkinson's disease. Int J Mol Sci 22:4676. https://doi.org/10.3390/ijms22094676
8. Ben Haim L, Rowitch DH (2017) Functional diversity of astrocytes in neural circuit regulation. Nat Rev Neurosci 18:31–41. https://doi.org/10.1038/nrn.2016.159
9. Berman SB, Hastings TG (1999) Dopamine oxidation alters mitochondrial respiration and induces permeability transition in brain mitochondria: implications for Parkinson's disease. J Neurochem 73:1127–1137. https://doi.org/10.1046/j.1471-4159.1999.0731127.x
10. Betarbet R, Sherer TB, Greenamyre JT (2002) Animal models of Parkinson's disease. BioEssays 24:308–318. https://doi.org/10.1002/bies.10067
11. Betarbet R, Sherer TB, MacKenzie G, Garcia-Osuna M, Panov AV, Greenamyre JT (2000) Chronic systemic pesticide exposure reproduces features of Parkinson's disease. Nat Neurosci 3:1301–1306. https://doi.org/10.1038/81834
12. Brandebura AN, Paumier A, Onur TS, Allen NJ (2023) Astrocyte contribution to dysfunction, risk and progression in neurodegenerative disorders. Nat Rev Neurosci 24:23–39. https://doi.org/10.1038/s41583-022-00641-1
13. Chung RS, Penkowa M, Dittmann J, King CE, Bartlett C, Asmussen JW et al (2008) Redefining the role of metallothionein within the injured brain: extracellular metallothioneins play an important role in the astrocyte-neuron response to injury. J Biol Chem 283:15349–15358. https://doi.org/10.1074/jbc.M708446200
14. Chung RS, West AK (2004) A role for extracellular metallothioneins in CNS injury and repair. Neuroscience 123:595–599. https://doi.org/10.1016/j.neuroscience.2003.10.019
15. De Biase LM, Schuebel KE, Fusfeld ZH, Jair K, Hawes IA, Cimbro R et al (2017) Local cues establish and maintain region-specific phenotypes of basal

ganglia microglia. Neuron 95:341–356. https://doi.org/10.1016/j.neuron.2017.06.020
16. Dhillon AS, Tarbutton GL, Levin JL, Plotkin GM, Lowry LK, Nalbone JT et al (2008) Pesticide/environmental exposures and Parkinson's disease in east Texas. J Agromed 13:37–48. https://doi.org/10.1080/10599240801986215
17. Emdadul Haque M, Asanuma M, Higashi Y, Miyazaki I, Tanaka K, Ogawa N (2003) Apoptosis-inducing neurotoxicity of dopamine and its metabolites via reactive quinone generation in neuroblastoma cells. Biochim Biophys Acta 1619:39–52. https://doi.org/10.1016/s0304-4165(02)00440-3
18. Gopinath A, Mackie PM, Phan LT, Tansey MG, Khoshbouei H (2023) The complex role of inflammation and gliotransmitters in Parkinson's disease. Neurobiol Dis 176:105940. https://doi.org/10.1016/j.nbd.2022.105940
19. Hamby ME, Uliasz TF, Hewett SJ, Hewett JA (2006) Characterization of an improved procedure for the removal of microglia from confluent monolayers of primary astrocytes. J Neurosci Methods 150:128–137. https://doi.org/10.1016/j.jneumeth.2005.06.016
20. Heneka MT, Rodriguez JJ, Verkhratsky A (2010) Neuroglia in neurodegeneration. Brain Res Rev 63:189–211. https://doi.org/10.1016/j.brainresrev.2009.11.004
21. Higashi Y, Segawa S, Matsuo T, Nakamura S, Kikkawa Y, Nishida K et al (2011) Microglial zinc uptake via zinc transporters induces ATP release and the activation of microglia. Glia 59:1933–1945. https://doi.org/10.1002/glia.21235
22. Johnson ME, Bobrovskaya L (2015) An update on the rotenone models of Parkinson's disease: their ability to reproduce the features of clinical disease and model gene-environment interactions. Neurotoxicology 46:101–116. https://doi.org/10.1016/j.neuro.2014.12.002
23. Kabba JA, Xu Y, Christian H, Ruan W, Chenai K, Xiang Y et al (2018) Microglia: housekeeper of the central nervous system. Cell Mol Neurobiol 38:53–71. https://doi.org/10.1007/s10571-017-0504-2
24. Kuhn DM, Arthur RE Jr, Thomas DM, Elferink LA (1999) Tyrosine hydroxylase is inactivated by catechol-quinones and converted to a redox-cycling quinoprotein: possible relevance to Parkinson's disease. J Neurochem 73:1309–1317. https://doi.org/10.1046/j.1471-4159.1999.0731309.x
25. Kuhn DM, Francescutti-Verbeem DM, Thomas DM (2006) Dopamine quinones activate microglia and induce a neurotoxic gene expression profile: relationship to methamphetamine-induced nerve ending damage. Ann NY Acad Sci 1074:31–41. https://doi.org/10.1196/annals.1369.003
26. LaVoie MJ, Ostaszewski BL, Weihofen A, Schlossmacher MG, Selkoe DJ (2005) Dopamine covalently modifies and functionally inactivates parkin. Nat Med 11:1214–1221. https://doi.org/10.1038/nm1314
27. Liddelow SA, Guttenplan KA, Clarke LE, Bennett FC, Bohlen CJ, Schirmer L et al (2017) Neurotoxic reactive astrocytes are induced by activated microglia. Nature 541:481–487. https://doi.org/10.1038/nature21029
28. Lobsiger CS, Cleveland DW (2007) Glial cells as intrinsic components of non-cell-autonomous neurodegenerative disease. Nat Neurosci 10:1355–1360. https://doi.org/10.1038/nn1988
29. Matyash V, Kettenmann H (2010) Heterogeneity in astrocyte morphology and physiology. Brain Res Rev 63:2–10. https://doi.org/10.1016/j.brainresrev.2009.12.001
30. Miyazaki I, Asanuma M (2008) Dopaminergic neuron-specific oxidative stress caused by dopamine itself. Acta Med Okayama 62:141–150. https://doi.org/10.18926/AMO/30942
31. Miyazaki I, Asanuma M, Hozumi H, Miyoshi K, Sogawa N (2007) Protective effects of metallothionein against dopamine quinone-induced dopaminergic neurotoxicity. FEBS Lett 581:5003–5008. https://doi.org/10.1016/j.febslet.2007.09.046
32. Miyazaki I, Asanuma M, Kikkawa Y, Takeshima M, Murakami S, Miyoshi K et al (2011) Astrocyte-derived metallothionein protects dopaminergic neurons from dopamine quinone toxicity. Glia 59:435–451. https://doi.org/10.1002/glia.21112
33. Miyazaki I, Asanuma M, Murakami S, Takeshima M, Torigoe N, Kitamura Y et al (2013) Targeting 5-HT(1A) receptors in astrocytes to protect dopaminergic neurons in Parkinsonian models. Neurobiol Dis 59:244–256. https://doi.org/10.1016/j.nbd.2013.08.003
34. Miyazaki I, Isooka N, Imafuku F, Sun J, Kikuoka R, Furukawa C et al (2020) Chronic systemic exposure to low-dose rotenone induced central and peripheral neuropathology and motor deficits in mice: reproducible animal model of Parkinson's disease. Int J Mol Sci 21:3254. https://doi.org/10.3390/ijms21093254
35. Miyazaki I, Murakami S, Torigoe N, Kitamura Y, Asanuma M (2016) Neuroprotective effects of levetiracetam target xCT in astrocytes in parkinsonian mice. J Neurochem 136:194–204. https://doi.org/10.1111/jnc.13405
36. Mullett SJ, Hinkle DA (2011) DJ-1 deficiency in astrocytes selectively enhances mitochondrial complex I inhibitor-induced neurotoxicity. J Neurochem 117:375–387. https://doi.org/10.1111/j.1471-4159.2011.07175.x
37. Pannasch U, Rouach N (2013) Emerging role for astroglial networks in information processing: from synapse to behavior. Trends Neurosci 36:405–417. https://doi.org/10.1016/j.tins.2013.04.004
38. Parameshwaran K, Irwin MH, Steliou K, Pinkert CA (2012) Protection by an antioxidant of rotenone-induced neuromotor decline, reactive oxygen species generation and cellular stress in mouse brain. Pharmacol Biochem Behav 101:487–492. https://doi.org/10.1016/j.pbb.2012.02.011
39. Paz MA, Fluckiger R, Boak A, Kagan HM, Gallop PM (1991) Specific detection of quinoproteins by redox-cycling staining. J Biol Chem 266:689–692. https://doi.org/10.1016/S0021-9258(17)35225-0
40. Penkowa M (2006) Metallothioneins are multipurpose neuroprotectants during brain pathology. FEBS J 273:1857–1870. https://doi.org/10.1111/j.1742-4658.2006.05207.x
41. Rao A, Luo C, Hogan PG (1997) Transcription factors of the NFAT family: regulation and function. Annu Rev Immunol 15:707–747. https://doi.org/10.1146/annurev.immunol.15.1.707
42. Robinson MB (1998) The family of sodium-dependent glutamate transporters: a focus on the GLT-1/EAAT2 subtype. Neurochem Int 33:479–491. https://doi.org/10.1016/s0197-0186(98)00055-2
43. Rock RB, Gekker G, Hu S, Sheng WS, Cheeran M, Lokensgard JR et al (2004) Role of microglia in central nervous system infections. Clin Microbiol Rev 17:942–964. https://doi.org/10.1128/CMR.17.4.942-964.2004
44. Rohl C, Sievers J (2005) Microglia is activated by astrocytes in trimethyltin intoxication. Toxicol Appl Pharmacol 204:36–45. https://doi.org/10.1016/j.taap.2004.08.007
45. Ryu S, Sidorov S, Ravussin E, Artyomov M, Iwasaki A, Wang A et al (2022) The matricellular protein SPARC induces inflammatory interferon-response in macrophages during aging. Immunity 55(1609–1626):e1607. https://doi.org/10.1016/j.immuni.2022.07.007
46. Sakka N, Sawada H, Izumi Y, Kume T, Katsuki H, Kaneko S et al (2003) Dopamine is involved in selectivity of dopaminergic neuronal death by rotenone. NeuroReport 14:2425–2428. https://doi.org/10.1097/01.wnr.0000099604.19426.06
47. Sanders LH, Timothy Greenamyre J (2013) Oxidative damage to macromolecules in human Parkinson disease and the rotenone model. Free Radic Biol Med 62:111–120. https://doi.org/10.1016/j.freeradbiomed.2013.01.003
48. Shih AY, Johnson DA, Wong G, Kraft AD, Jiang L, Erb H et al (2003) Coordinate regulation of glutathione biosynthesis and release by Nrf2-expressing glia potently protects neurons from oxidative stress. J Neurosci 23:3394–3406. https://doi.org/10.1523/JNEUROSCI.23-08-03394.2003
49. Sidoryk-Wegrzynowicz M, Wegrzynowicz M, Lee E, Bowman AB, Aschner M (2011) Role of astrocytes in brain function and disease. Toxicol Pathol 39:115–123. https://doi.org/10.1177/0192623310385254
50. Solano RM, Casarejos MJ, Menendez-Cuervo J, Rodriguez-Navarro JA, Garcia de Yebenes J, Mena MA (2008) Glial dysfunction in parkin null mice: effects of aging. J Neurosci 28:598–611. https://doi.org/10.1523/JNEUROSCI.4609-07.2008
51. Soudani N, Ghantous CM, Farhat Z, Shebaby WN, Zibara K, Zeidan A (2016) Calcineurin/NFAT activation-dependence of leptin synthesis and vascular growth in response to mechanical stretch. Front Physiol 7:433. https://doi.org/10.3389/fphys.2016.00433
52. Stephenson EL, Jain RW, Ghorbani S, Gorter RP, D'Mello C, Yong VW (2024) Uncovering novel extracellular matrix transcriptome alterations in lesions of multiple sclerosis. Int J Mol Sci 25:1240. https://doi.org/10.3390/ijms25021240
53. Tietze F (1969) Enzymic method for quantitative determination of nanogram amounts of total and oxidized glutathione: applications to mammalian blood and other tissues. Anal Biochem 27:502–522. https://doi.org/10.1016/0003-2697(69)90064-5
54. Uriarte Huarte O, Kyriakis D, Heurtaux T, Pires-Afonso Y, Grzyb K, Halder R et al (2021) Single-cell transcriptomics and in situ morphological analyses reveal microglia heterogeneity across the nigrostriatal pathway. Front Immunol 12:639613. https://doi.org/10.3389/fimmu.2021.639613
55. Wang XF, Cynader MS (2000) Astrocytes provide cysteine to neurons by releasing glutathione. J Neurochem 74:1434–1442. https://doi.org/10.1046/j.1471-4159.2000.0741434.x
56. Whitehead RE, Ferrer JV, Javitch JA, Justice JB (2001) Reaction of oxidized dopamine with endogenous cysteine residues in the human dopamine transporter. J Neurochem 76:1242–1251

57. Xue J, Thippegowda PB, Hu G, Bachmaier K, Christman JW, Malik AB et al (2009) NF-kappaB regulates thrombin-induced ICAM-1 gene expression in cooperation with NFAT by binding to the intronic NF-kappaB site in the ICAM-1 gene. Physiol Genomics 38:42–53. https://doi.org/10.1152/physiolgenomics.00012.2009
58. Zhou ZD, Lim TM (2009) Dopamine (DA) induced irreversible proteasome inhibition via DA derived quinones. Free Radic Res 43:417–430. https://doi.org/10.1080/10715760902801533

## Publisher's Note